Australian Government
Bureau of Meteorology

bushfire&natural HAZARDSCRC

FINAL PROJECT REPORT
bnhcrc.com.au

MITIGATING THE EFFECTS OF SEVERE FIRES, FLOODS AND HEATWAVES THROUGH THE IMPROVEMENTS OF LAND DRYNESS MEASURES AND FORECASTS

Final project report

Vinodkumar, Imitaz Dharssi and Paul Fox-Hughes
Bureau of Meteorology & Bushfire and Natural Hazards CRC

Version	Release history	Date
1.0	Initial release of document	08/022021

© Bushfire and Natural Hazards CRC 2021

All material in this document, except as identified below, is licensed under the Creative Commons Attribution-Non-Commercial 4.0 International Licence.

Material not licensed under the Creative Commons licence:

- Department of Industry, Science, Energy and Resources logo
- Cooperative Research Centres Program logo
- Bushfire and Natural Hazards CRC logo
- Any other logos
- All photographs, graphics and figures

All content not licenced under the Creative Commons licence is all rights reserved. Permission must be sought from the copyright owner to use this material.

Disclaimer:
The Bureau of Meteorology and the Bushfire and Natural Hazards CRC advise that the information contained in this publication comprises general statements based on scientific research. The reader is advised and needs to be aware that such information may be incomplete or unable to be used in any specific situation. No reliance or actions must therefore be made on that information without seeking prior expert professional, scientific and technical advice. To the extent permitted by law, the Bureau of Meteorology and the Bushfire and Natural Hazards CRC (including its employees and consultants) exclude all liability to any person for any consequences, including but not limited to all losses, damages, costs, expenses and any other compensation, arising directly or indirectly from using this publication (in part or in whole) and any information or material contained in it.

Publisher:
Bushfire and Natural Hazards CRC

February 2021

Citation: Kumar V, Dharssi I, Fox-Hughes P (2021) Mitigating the effects of severe fire, floods and heatwaves through the improvements of land dryness measures and forecasts - final project report, Bushfire and Natural Hazards CRC, Melbourne.

Cover: Dry Earth. Source: pxhere (https://pxhere.com/en/photo/561747)

TABLE OF CONTENTS

ACKNOWLEDGMENTS

The support of the Commonwealth of Australia through the Bushfire and Natural Hazards Cooperative Research Centre program is acknowledged. We thank our end-users for their support and encouragement throughout the project period. We acknowledge our colleagues in the Bureau, particularly in the Earth System Modelling program, who helped us with various aspects of our project. We would especially like to place our gratitude on record to (not in any particular order) Pete Steinle, Beth Ebert, Jeff Kepert, John Bally (now at AFAC), Andrew Frost, Evan Morgan, Chun-Hsu Su, Robert Smalley, Huqiang Zhang, Monika Krysta, Shaun Cooper, Robin Bowen, Duan Beckett, Wenming Lu and Milton Woods for their support at various times for the successful completion of the project. We are also grateful to our colleagues Chun-Hsu Su and Nathan Eizenberg for providing atmospheric reanalysis data. The authors thank CSIRO for CosmOz data, University of Melbourne and Monash University for OzNet observations and TERN-OzFlux facility for OzFlux data. We also thank EUMETSAT, CATDS and NASA for ASCAT, SMOS and MODIS FRP data respectively. We are grateful to Dr Marta Yebra of Australian National University for the live fuel moisture content dataset.

EXECUTIVE SUMMARY

This Bushfire and Natural Hazards CRC project, titled *Mitigating the effects of severe fires, floods and heatwaves through the improvements of land dryness measures and forecasts*, was a partnership with the Bureau of Meteorology, and examined the use of detailed land surface models, satellite measurements and ground-based observations for the monitoring and prediction of landscape dryness. This project addresses a fundamental limitation in our ability to prepare for fires, floods and heatwaves and is directly linked to pre-event planning as well as forecasting of events. The research conducted in the present project solely focuses on the application of soil and land dryness/moisture in the context of fire danger and fire management practices. The lack of focus on flood and heatwave is circumstantial. The research priorities were set and driven by the requirements of the project end-users, all of them from various fire management agencies across Australia. Hence, the end-use interest was solely on the application of the research in fire management. Nevertheless, it is worth pointing that there is a substantial amount of research literature which establishes the importance of soil moisture in flood and heatwave prediction and applications.

Currently, landscape dryness for fire management is estimated in Australia using simple empirical models developed in the 1960s. The most prominent of those used in Australia are the Keetch-Byram Drought Index (KBDI) and the Soil Dryness Index (SDI). An initial study performed as part of this project suggested that analyses of soil moisture can be improved by using physics-based land surface models, remote sensing measurements and data assimilation.

JASMIN prototype

To address this, the present project developed a standalone prototype land surface modelling system, called Joint UK Land Environment Simulator based Australian Soil Moisture Information (JASMIN) to produce daily soil moisture analyses at 5km resolution and 4 soil layers. Verification against ground-based soil moisture observations shows that this prototype system is significantly more skilful than both KBDI and SDI.

Though JASMIN can supplement many applications that require accurate soil moisture estimates, the biggest beneficiary of this new system will be the fire agencies. The soil moisture estimate from the new system provides a robust alternative to the methods currently used in fire prediction. This is evident from the verifications performed against in situ measurements. KBDI and SDI show large errors over regions where they are used operationally. KBDI, for example, has a large wet bias over southern regions that could undermine fire danger ratings. The JASMIN system can produce reliable soil moisture information over a wide range of land-use types, which potentially extends its applicability to other fields as well. Also, JASMIN is shown to have good skill for both surface and deep soil horizons.

JASMIN calibration

To promote an effective adoption of JASMIN in current operational practices, calibration methods were applied to the native JASMIN soil moisture datasets. The key aim of these methods was to calibrate JASMIN outputs in units of moisture excess to moisture deficit values that range from 0–200, as required by McArthur's

Forest Fire Danger Index (FFDI; McArthur, 1967). The calibration offers a simple, faster and cost-effective way to make significant upgrades to the existing operational systems used by fire and other environmental agencies.

The calibration methods applied were minimum-maximum matching, mean-variance matching, and cumulative distribution function matching. The selection of these calibration methods was based on the potential end-user requirement, whether that is to simply replace the legacy systems with a new product with high skill (e.g., minimum-maximum method), or to replace the existing system that captures the temporal variations better while preserving the climatology of the older system (e.g., mean-variance and cumulative distribution function matching). The latter could be useful if existing operating systems are already tuned to offset the bias in the current soil moisture deficit methods.

Improving high spatial resolution mapping

This project also aimed to improve applications such as fire danger mapping that may require soil moisture information at higher spatial resolution due to the large spatial variability of soil moisture in the landscape. A common practice to overcome such a problem is to employ downscaling methods to increase the spatial scale of the product. Recent advances in optical remote sensing have allowed researchers to use different remote sensing products that reflect soil moisture variability as ancillary information. A method based on a "universal triangle" concept is used in several previous studies, which establishes a relationship between soil moisture, vegetation index, and surface radiant temperature from optical remote sensing. This project applied three downscaling methodologies: two based on regression and one based on a physics-based approach.

Results from the downscaling methodologies indicate that it is feasible to improve the spatial resolution of JASMIN using all three disaggregating algorithms and preserve the general large-scale spatial structure seen in JASMIN soil moisture estimates. However, the seasonal means obtained at 1 km show that each product displays characteristic soil moisture spatial variability at fine scales. Results from the comparison with ground-based soil moisture measurements indicate that there is no significant degradation of the bias in the three methods when moving to higher spatial resolution.

Predicting live fuel moisture content

Prediction of the moisture status in live fuels is an important gap in current fire management practices which, if filled, can potentially be useful for spatial and temporal assessment of landscape dryness. The final objective of the project was thus to explore the relationship between soil moisture and live fuel moisture content (LFMC) using the datasets from JASMIN and Australian Flammability Monitoring System (AFMS), respectively. The analysis carried out indicates that soil moisture is a leading indicator of LFMC. This project developed a simple yet skilful model to predict live fuel moisture content for the whole of Australia.

The key variable is the 0-350 mm layer soil moisture derived from the JASMIN system. The modelling strategy pursued consists of a linear combination of two sub-models: one to capture the annual cycle and one to capture the daily variations. A time function represents the LFMC annual cycle model. The daily deviations in LFMC are captured by using a linear regression model with 14-day lagged daily deviations in soil moisture as the input. The daily changes in soil moisture are computed by deviations from its annual cycle.

When evaluated over 60 sites, the approach returned an average R^2 of 0.64 with normalised root mean square error values of <25% at all sites. As researchers were employing a gridded soil moisture product, this strategy facilitates the reconstruction of past events, as well as data gap filling. The lag of 14 days implies a lead time of 14 days for predicting the LFMC. This has significant operational implications, as daily variations in LFMC can be predicted using soil moisture information from JASMIN on a national scale.

JASMIN is currently run as a prototype research system, with soil moisture analysis done only near-real-time. However, JASMIN can be extended to produce both real-time analysis and forecasts. The prognostic mode can provide soil moisture forecasts for up to 10 days. This means a maximum lead time of 24 days can be achieved by utilising soil moisture forecasts.

JASMIN utilisation

A key focus of the project from its inception was to create pathways for easier utilisation of the project deliverables. This is reflected in both the scientific and technical approaches adopted in this project. For example, the calibration of JASMIN to KBDI and SDI was done to facilitate the ready utilisation of JASMIN in the existing operational system. A total of 8 calibrated JASMIN soil dryness products were developed and made available through the Bureau of Meteorology's THREDDS server. The JASMIN soil moisture in volumetric units at 4 layers are also provided via the THREDDS server for interested parties to evaluate. The volumetric soil moisture fields from the top two JASMIN layers (0-100 mm and 100-350 mm) are available via AFMS as well.

The datasets on both THREDDS and AFMS are updated near-real-time. There is a continuing interest in the end-user community in utilising JASMIN for various fire management applications. In that respect, JASMIN has been assessed in the Western Australian Department of Biodiversity, Conservation and Attractions study on tall wet forest fuel availability. Tasmania Parks and Wildlife has also been using JASMIN as a decision-support tool to restrict the use of open fires in national parks. Also, JASMIN data were updated specifically to assist with Tasmanian decision-making for 2018-19 seasonal bushfire assessment workshop and preseason consultative committee on fire weather.

The JASMIN system can produce reliable soil moisture estimates over a wide range of land-use types and can support many applications that require accurate soil moisture information. However, there is still scope for improvements to the JASMIN system, whether it be the skill or the scale.

An immediate focus could be the use of data assimilation techniques to improve the skill of JASMIN. Data assimilation allows uncertainties in land surface model soil moisture to be offset to some extent by routinely updating the hydrological conditions using the information provided by observations on state variables used by land surface models. The assimilation of satellite observations is shown to improve the model soil moisture state. In that respect, the use of NASA's land information system (LIS) is being evaluated at the Bureau. The LIS is a complex framework that uses extensible interfaces to allow the incorporation of new domains, land surface models, land surface parameters, meteorological inputs, data assimilation and optimisation algorithms. The extensible nature of these interfaces, and the component style specifications of the system, allow rapid prototyping and development of new applications. The JASMIN system can be incorporated within LIS to facilitate the assimilation of various observation types. Further, it can be leveraged to run JASMIN with an enhanced spatial resolution, desirably at 1 km.

END-USER PROJECT IMPACT STATEMENT

Mark Chladil, *Fire Management Planning Officer, Tasmania Fire Service, TAS*

This project sought to provide an improved characterisation of soil moisture to better inform forecasting of fires, floods and heatwaves as well as assisting the management of planned fires and bushfires. The approach is well suited to the current observational and forecasting systems and has applicability to a wide range of surface cover types and climates and JASMIN has already been shown to give reliable soil moisture estimates for multiple levels at relatively fine scale. I have been using the Mount Soil Dryness Index (SDI) for close to 40 years and it was gratifying that the research showed that the Mount SDI was superior to the Keetch-Byram Drought Index (KBDI). This verified the work done by Tony Mount in the late '60s and through the '70s to build on the work of John Keetch and George Byram to account for evaporative losses from forests and better represent the hydrology and thus improve fuel moisture information. The researchers have also provided calibration of JASMIN volumetric output to both SDI and KBDI to allow end-users such as fire managers to see and think about the ways the numbers change through time for their areas of interest. The influence of soil moisture on live fuel moisture has been explored so that JASMIN is able to provide information on this minor and generally overlooked fuel fraction. Thankfully JASMIN has been developed with the capacity to be readily downscaled (to the kilometre level!) and to use the improving land surface models, especially NASA's Land Information System (LIS) so the both the skill and scale of JASMIN will continue to improve as these other models are themselves improved. This has been a long road and the researchers and project managers have delivered good outcomes and a way forward. Of course, much can be done in the way of additional research and development, but the bigger challenge now is for agencies to bring JASMIN into their practices and to exploit the additional data richness and finer spatial scales.

PRODUCT USER TESTIMONIALS

David Taylor, *Parks and Wildlife Service, Department of Primary Industry, Parks, Water and Environment, TAS*

We use the outputs of this project in both in our Planned Burn and Bushfire Operations. In planned burn operations it used to assist in identifying potential areas of concerns for organic soil combustion and in bushfire preparedness it is used to identifying areas for potential holdover fires that could occur during active lightning periods in which we can direct patrols and or spotter flights.

INTRODUCTION

Good estimates of landscape dryness underpin fire danger rating, fire behaviour models, flood prediction and landslip warning. Soil dryness also strongly influences heatwave development by driving the transfer of solar heating from the soil surface into air. Fire intensity, spread rate, and ignition are very sensitive to the fuel dryness, which is strongly linked to soil moisture content. For example, Nolan et al. (2016) highlighted clear thresholds of fuel moisture content linked with wildfire occurrences in forests and woodlands. Gellie et al. (2010) showed that the occurrence of large destructive fires corresponds to very large soil moisture deficit (SMD) values. Estimates and forecasts of fuel and/or soil moisture (SM) are used to assess wildfire risks and to warn of developing fire danger. SM products are also an essential ingredient for forecasting river flows on seasonal scales (one to three months), which is very much in demand by water managers and reservoir operators.

Modern, state of the art land surface models (LSMs) calculates landscape dryness with greater sophistication and account for details such as soil texture, solar insolation, root depth, vegetation type and stomatal resistance. The Australian Community Climate and Earth System Simulator (ACCESS) model has four soil layers. The topmost layer from the surface to 100 mm is critical for the exchange of moisture between the soil and forest litter fuels. The deepest layer extends down to 3 metres.

Currently, landscape dryness is estimated using very crude models developed in the 1960s. The most prominent of those used in Australia are the Keetch-Byram Drought Index (KBDI; Keetch and Byram, 1968) developed by the US Forest Service, and the related Soil Dryness Index (SDI; Mount, 1972) developed by Forestry Tasmania. These simple empirical SM models are designed for easy hand calculation once per day for a small number of points across the landscape. These empirical calculators do not work effectively in drier environments, which are typical in the Australian landscape and are predicted to become more widespread as the climate changes. They do not consider different soil types, slope, aspect, and many other factors. They are poor drivers of the fire models used by fire agencies and the Bureau of Meteorology to manage and warn for dangerous fire conditions as the science is outdated and has been verified as not effective in fire spread prediction.

This project addresses a fundamental limitation in our ability to prepare for fires, floods and heatwaves and is directly linked to pre-event planning as well as forecasting of events. Both aspects are core elements of a resilient community. The outputs of this project can improve Australia's ability to manage extreme events by developing a state of the art, world's best practice in SM analysis that makes use of many different sources of observations and cutting-edge land surface modelling and data assimilation. The research examines the use of detailed land surface models, remotely sensed satellite measurements and ground-based observations for the monitoring and prediction of landscape dryness.

There are few in-situ observations of SM. However, several new satellite systems have been launched that can provide information about surface SM. The advantage of these satellite systems is that they provide national coverage on a daily timescale. Advanced land data assimilation schemes can be used to blend the satellite measurements with model forecasts.

The potential benefits of this project are:

- More accurate, detailed, and confident estimates and forecasts of SM, and hence an expectation of more accurate predictions of fire risk, flood forecasting, landslip warning and heatwave events.
- The research can potentially benefit landscape and fire management applications including assessments for fuel reduction burns.
- Benefits extend to water resource management, dam catchment monitoring and function of dams in flood mitigation.
- Datasets of landscape dryness can support a wide range of other research in fire, flood, and heatwave prediction.

BACKGROUND

The KBDI and SDI are found to have limited skill in estimating SM, particularly in shallow soil layers (Vinodkumar et al., 2017). The dependency of fire potential on moisture in a layer of soil may change with seasons (Haines et al., 1976). A good SM estimation system should, therefore, work throughout the seasons and should not depend upon a fixed depth of soil horizon (like KBDI and SDI) to indicate fire danger. A model system employing a multi-layer soil model is suggested to be the best solution (Haines et al., 1976). Land surface modelling is an emerging technology that could potentially fill this gap. LSMs are capable of estimating soil moisture at different layers and more systematically than empirical methods.

A prototype high-resolution SM information system based on Joint UK Land Environment Simulator (JULES; Best et al., 2011) LSM to estimate SM has been developed (Dharssi and Vinodkumar, 2017). This system is called the JULES based Australian Soil Moisture Information (JASMIN) and estimates SM at a spatial resolution of 5 km. JASMIN provides information at four soil layers, with a 100 mm thick surface layer and a soil column of 3 m thickness to represent the root-zone. Verification against ground-based SM observations shows that this prototype system is significantly better than the simple KBDI and SDI models currently used operationally (Dharssi and Vinodkumar, 2017).

The main achievements of the project include:

1. Production of a historical dataset of the KBDI and SDI at 5 km horizontal resolution using analyses of rainfall and maximum temperature.
2. Inter-comparison of traditional soil dryness models (KBDI, SDI) with soil moisture/dryness from:
    a) Numerical Weather Prediction models (ACCESS and others).
    b) Satellite-based measures of landscape dryness.
    c) Ground-based SM observations.
3. Development, production, and validation of the JASMIN system.
4. Calibration of JASMIN SM for utilization in current operational fire prediction systems.
5. Release of historical JASMIN datasets and near-real-time updates through the Australian Flammability Monitoring System and Bureau's THREDDS server.
6. Downscaling of JASMIN SM from 5 km to 1 km spatial resolution.
7. Development of a simple LFMC predictive model based on SM.

RESEARCH APPROACH

The main research components of the project and the scientific approaches undertaken in each component are described below.

DEVELOPMENT AND VALIDATION OF JASMIN SYSTEM

JASMIN system

Land surface modelling has become a great tool in continually estimating SM at large scales, where mapping with the use of in-situ observations becomes non-feasible. Land surface models (LSMs) represent processes which regulate the exchanges of water and energy through the soil-plant-atmosphere continuum. There is a lack of an operational, high-resolution land surface modelling system for Australia that can analyse various components of the surface energy and water balance. The analyses of energy and water balance produced by operational numerical weather prediction (NWP) are at a low resolution (~18 km). Further, land surface products from NWP may have limited skill due to the large uncertainties that exist in NWP forcing, especially precipitation. There are operational water balance models run by the Bureau of Meteorology (BoM) that can provide estimates of SM at a higher resolution. However, most of these models are designed and calibrated towards some very specific applications (e.g. streamflow and catchment water balance assessment). Moreover, the energy balance in these hydrological models is simplified. These factors could limit their ability to simulate an accurate estimate of SM, especially at top layers. In light of the lack of a comprehensive system to analyse SM in particular and land surface variables in general, a stand-alone high-resolution land surface modelling system was developed.

The land surface in JASMIN/JULES is divided into grids, and each grid box is divided further into fractions of different surface types (called tiles) to represent land cover heterogeneity. Nine surface tiles are defined: five plant functional types (PFTs) – broad-leaf trees, needle-leaf trees, C3 grasses, C4 grasses, and shrubs; and four non-vegetation types - urban, inland water, bare soil, and ice. A multi-layer soil profile can be defined for each grid box, where the soil is vertically homogeneous. The change in total soil moisture content (SMC) within each soil layer from the previous time step is based on the evapotranspiration (ET) extracted directly from the layer by plant roots, the diffusive water flux flowing in from the layer above, and the diffusive flux flowing out to the layer below (Cox et al., 1999). The SM tendency is based on a finite difference approximation of Richards's equation and Darcy's law. JULES has an option to use the soil hydraulic models of either Brooks and Corey (1964) or van Genuchten (1980). JASMIN uses the van Genuchten soil hydraulic model to define the relationship between SM and soil hydraulic conductivity. Transpiration by plants extracts soil water directly from the soil layers via the plant roots while bare soil evaporation extracts soil water from the topmost soil layer only. The ability of plants to access water from each soil layer is determined by the root density distribution and SM availability. The SM availability is a function of SM and soil texture. ET is modelled using a modified Penman/Monteith equation coupled to a photosynthesis/surface conductance model. JULES use ancillary information on land cover types, vegetation heights, soil texture, soil albedo, soil hydraulic and thermal properties, leaf area index (LAI) etc. The LAI ancillary information is seasonally varying whereas vegetation properties like height, land cover etc. are static. JULES provides numerous variables describing the state of the land-surface in terms of water, energy, and carbon fluxes as outputs.

The JASMIN system covers the whole of Australia at a spatial resolution of 5 km. The system runs with an hourly time step and output is stored at every third timestep. The soil column in JASMIN is 3 m deep and is divided into four layers of 0.1, 0.35, 0.65 and 2 m thickness successively from the surface. A canopy height dataset derived from space-borne light detection and ranging (LIDAR) instrument (Simard et al., 2011) is used for an accurate representation of tree heights in Australia. The tree height ancillaries are found to have a significant impact on model results (Dharssi et al., 2015).

The physical processes in LSMs are driven by meteorological data, and the frequencies by which the state variables are updated correspond to the temporal resolution of provided meteorological fields. The air temperature, specific humidity, wind speed and surface pressure data required by JASMIN is obtained from BoM's Mesoscale Surface Analysis System (MSAS; Glowacki et al., 2012). MSAS performs hourly analyses of atmospheric pressure at mean sea level, potential temperature, 2 m dew point temperature, and 10 m wind components on a ~4 km grid. This data is converted and re-gridded to drive JASMIN. The MSAS data is available from 2007 onwards and is on-going with near-real-time (NRT) updates. The downward surface shortwave radiation required by JULES is provided by an hourly product developed in the Bureau of Meteorology based on measurements from the Himawari geostationary meteorological satellites. This product is available at a spatial resolution of 5 km. The downward surface longwave radiation data is obtained from the Bureau of Meteorology's operational regional NWP model (Puri et al. 2013. The NWP data is available in NRT, 6-hourly at a resolution of 12 km. The precipitation data used to drive JASMIN is obtained from BoM's Australian Water Availability Project (AWAP; Jones et al. 2009) product. AWAP is an in-situ observation-based product and provides daily analyses of rainfall at a spatial resolution of ~5km. The Tropical Rainfall Measuring Mission (TRMM; Huffman et al. 2007) data is used to disaggregate AWAP rainfall to 3-hourly values. The TRMM data is also used to fill spatial gaps in the AWAP data.

Verification metrics

All the ground-based verification and evaluation in the present project was conducted over the well-known CosmOz (Hawdon et al., 2014), OzNet (Smith et al., 2012) and OzFlux (Beringer et al., 2016) SM networks in Australia (Figure 1). The three networks together comprise of about 60 sites spanning across the whole country and sample the climatic zones and vegetation types typical of the Australian landscape.

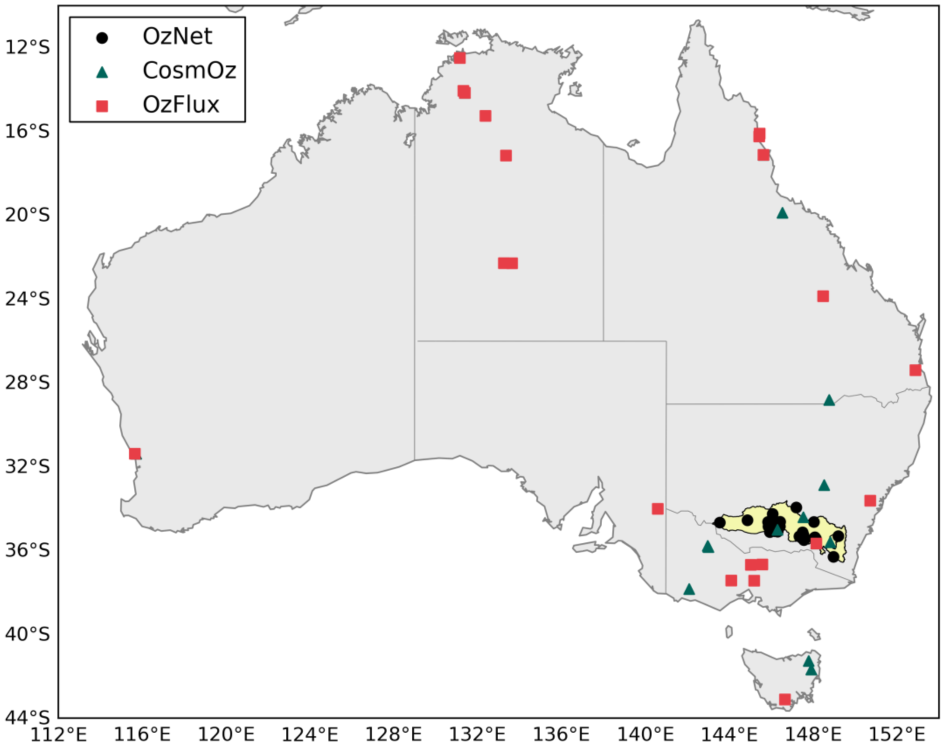

FIGURE 1. LOCATION OF IN-SITU OBSERVATIONS. THE REGION SHADED BY YELLOW REPRESENTS THE MURRUMBIDGEE CATCHMENT.

For verification conducted throughout the project, we adopted two popular schools of thoughts found in the literature. The first assumes an exact correspondence between SM from ground-based point observations and coarser model/satellite products. This approach is based on the temporal stability argument (Brocca et al., 2014), where it is assumed that the large fraction of SM spatial variability is time-invariant. The common metrics used in such studies, i.e., Pearson's product-moment correlation (R), unbiased root mean square difference (*ub*RMSD) and bias are calculated. The scores are computed for all stations and the whole period were comparing data overlaps. Only scores for significant correlations with p-values < 0.001 are presented. The equations for each of the above-mentioned metrics are given below.

$$\mathrm{R} = \frac{\frac{1}{N}\sum_{i=1}^{N}(\widehat{\Theta}^{i}_{\mathrm{model}}-\overline{\widehat{\Theta}_{\mathrm{model}}})(\widehat{\Theta}^{i}_{\mathrm{insitu}}-\overline{\widehat{\Theta}_{\mathrm{insitu}}})}{\sigma_{\mathrm{model}}\sigma_{\mathrm{in\ situ}}} \quad (1)$$

$$\mathrm{RMSD} = \sqrt{\frac{1}{N}\sum_{i=1}^{N}(\widehat{\Theta}^{i}_{\mathrm{insitu}}-\widehat{\Theta}^{i}_{\mathrm{model}})^2} \quad (2)$$

$$\mathrm{Bias} = \frac{1}{N}\sum_{i=1}^{N}(\widehat{\Theta}^{i}_{\mathrm{insitu}}-\widehat{\Theta}^{i}_{\mathrm{model}}) \quad (3)$$

$$\mathrm{ubRMSD} = \sqrt{\mathrm{RMSD}^2-\mathrm{Bias}^2} \quad (4)$$

where $\hat{\theta}$ is the SM and σ is the standard deviation.

To calculate correlations with seasonal effects removed, we compute the anomalies for each dataset using:

$$\hat{\theta}_{an} = \widehat{\Theta} - \hat{\theta}_{av} \quad (5)$$

$\hat{\Theta}_{av}$ is the mean and is calculated over a 31-day sliding window. Fisher's transformation is applied to calculate the average correlation (Corey et al., 1998).

The second school of thought argues that the assumption of ground-based observation as "truth" is problematic, as they are imperfect due to their measurement errors and possibly have a support scale different to that required for the application in question. A host of SM verification studies have hence used a technique called Triple collocation (TC; Stoffelen, 1998) where none of the comparing datasets is treated as "truth". TC also has the advantage of not requiring the rescaling step, which may bias the error estimates (Yilmaz & Crow, 2013). TC estimates the random error variances of three collocated datasets which represent the same geophysical variable. These "triplets" are assumed to be mutually independent and their errors uncorrelated with each other and with the target geophysical variable. SM products from *in situ* observation, satellite remote sensing and land surface model are generally used triplets to compute TC statistics. TC has been used widely in SM verification studies (e.g. Dorigo et al., 2010; Miralles et al., 2010). McColl et al. (2014) extended the TC method to estimate the correlation coefficient of each measurement system to the unknown target variable. They called this approach Extended Triple Collocation (ETC). In the present study, we use the ETC method to estimate both correlations and error variances of each dataset. The error standard deviation for ETC is given by:

$$\sigma_\varepsilon = \begin{bmatrix} \sqrt{Q_{11} - \frac{Q_{12}Q_{13}}{Q_{23}}} \\ \sqrt{Q_{22} - \frac{Q_{12}Q_{23}}{Q_{13}}} \\ \sqrt{Q_{33} - \frac{Q_{13}Q_{23}}{Q_{12}}} \end{bmatrix} \quad (6)$$

Here Q_{ij} is the covariance between time series *i* and *j*. The correlation coefficient between truth "t" and estimate X is given by:

$$\rho_{t,X} = \pm \begin{bmatrix} \sqrt{\frac{Q_{12}Q_{13}}{Q_{11}Q_{23}}} \\ sign(Q_{13}Q_{23})\sqrt{\frac{Q_{12}Q_{23}}{Q_{22}Q_{13}}} \\ sign(Q_{12}Q_{23})\sqrt{\frac{Q_{13}Q_{23}}{Q_{33}Q_{12}}} \end{bmatrix} \quad (7)$$

where the $\rho_{t,X}$ is correct up to a sign ambiguity.

CALIBRATION OF JASMIN

The JULES LSM simulates SM in units of mass per unit area (kg m^{-2}). However, the drought factor (DF) calculations in FFDI requires SM deficit values specified in a range between 0 – 200. Hence the use of appropriate rescaling techniques is required to use JASMIN SM in the current operational DF calculations. The calibration exercise is an important step towards faster adoption of JASMIN product for operational use. Considering the significant resources required to adopt any new source of information in operations, the calibration provides an opportunity to make a significant improvement to the existing system with the least effort. The present study applied four rescaling methods to scale JASMIN SM to SMD values that range from 0 – 200. The scaling methods evaluated here are the minimum-maximum matching, mean-variance matching and cumulative distribution function (CDF) matching. Each of these methods is detailed below.

Rescaling methods

Minimum-maximum matching

The first approach involves rescaling JASMIN time series to match its minimum (Θ_{min}) and maximum (Θ_{max}) to those of SMD in FFDI (ϑ_{min} = 0, ϑ_{max} = 200).

$$\hat{\Theta} = \vartheta_{min} + (\Theta - \Theta_{min})(\frac{\vartheta_{max}-\vartheta_{min}}{\Theta_{max}-\Theta_{min}}) \quad (8)$$

This is mathematically equivalent to the approach by Albergel et al. (2012) and Vinodkumar et al. (2017), where they normalised SM data sets to a standard range 0 – 1. We refer to this approach as minimum-maximum (MM) matching.

Mean-variance matching

In the second approach, JASMIN data (Θ) is normalised ($\hat{\Theta}$) to have the same mean (μ) and variance (σ^2) as the reference (KBDI/SDI) data (ϑ). This is achieved through,

$$\hat{\Theta} = \mu_\vartheta + \frac{\sigma_\vartheta}{\sigma_\Theta}(\Theta - \mu_\Theta) \quad (9)$$

We denote this method as the μ - σ matching.

CDF matching

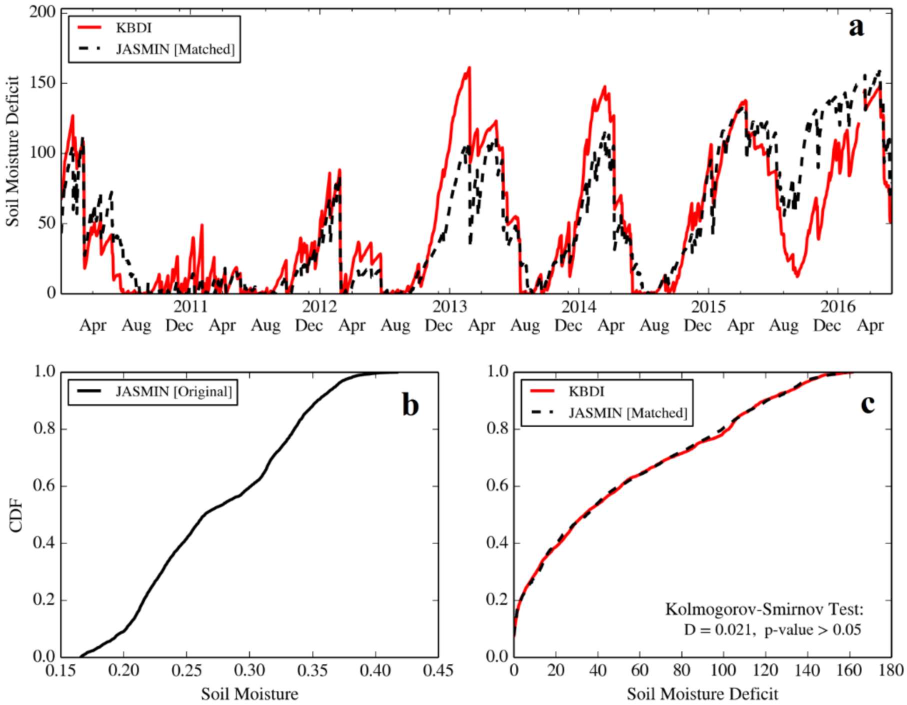

FIGURE 2. CDF MATCHING OVER RIGGS CREEK, QLD. (A) TIME SERIES OF KBDI (RED LINE) AND JASMIN (DASHED BLACK LINE) MATCHED TO KBDI SCALE. (B) CDF OF JASMIN SM IN VOLUMETRIC UNITS. (C) CDF OF KBDI (RED LINE) AND MATCHED JASMIN SMD (DASHED BLACK LINE).

The cumulative distribution function (CDF) matching (Reichle & Koster, 2004) is a nonlinear method that matches higher-order statistical moments of the distributions in addition to the mean and variance. The CDF characterises the cumulative probability of a continuous random variable (X) up to a specific value (x). That is,

$$F(x) = \Pr[X \leq x] \quad (10)$$

In CDF matching, the two datasets are ranked first and an operator, which is the best fit, is calculated. The ranking of datasets is performed on both temporal and spatial samples. The first is referred to as temporal CDF matching (tCDF) and the latter as spatial CDF matching (sCDF). The operator for tCDF is a ninth order polynomial fit of ranked JASMIN SM values to ranked KBDI/SDI values. The operator in tCDF is derived using the training data sets extending from 1st January 2010 to 31st December 2015. The best fit in sCDF is calculated using daily values over the entire JASMIN domain (-45° S to -10° S; 112° E to 154° E). The operator in sCDF is a cubic spline fit of ranked JASMIN SM values to ranked KBDI/SDI values. The sCDF technique is widely used in image processing where the contrast of an image is adjusted to a reference image.

Figure 2 shows an example of the CDF matching procedure for a time series over one location. The red line in Figure 2a depicts the KBDI and the black line represents JASMIN matched to KBDI. The black line in Figure 2b shows the CDF of JASMIN SM in volumetric units. Figure 2c shows the CDF of KBDI (red line) and matched JASMIN SMD (dashed black line).

DOWNSCALING OF JASMIN

Though JASMIN provides accurate SM information at high spatial resolution, it is at a coarser scale than is ideal for fire and other environmental applications. A common practice to overcome such a problem is to employ downscaling methods to increase the spatial scale of the product. Downscaling methods establish a functional relationship between SM and associated feature variables (e.g., topography, land-use, land surface temperature), whose spatial distribution can more readily be measured. The downscaling methods generally differ in the type of auxiliary input data (e.g., optical/thermal data, elevation/slope, soil attributes) and the characteristics of the disaggregation method (i.e., physics-based, or statistical). One of the most common and early frameworks used in SM downscaling is the use of landscape indices, especially terrain indices, to downscale the coarser-resolution SM data. However, the downscaling methods using terrain attributes often establish relationships by using extensive in-situ observations. Such methods are found to be catchment-specific, restricting their applicability to smaller spatial scales (Busch et al., 2012; Werbylo and Niemann, 2014).

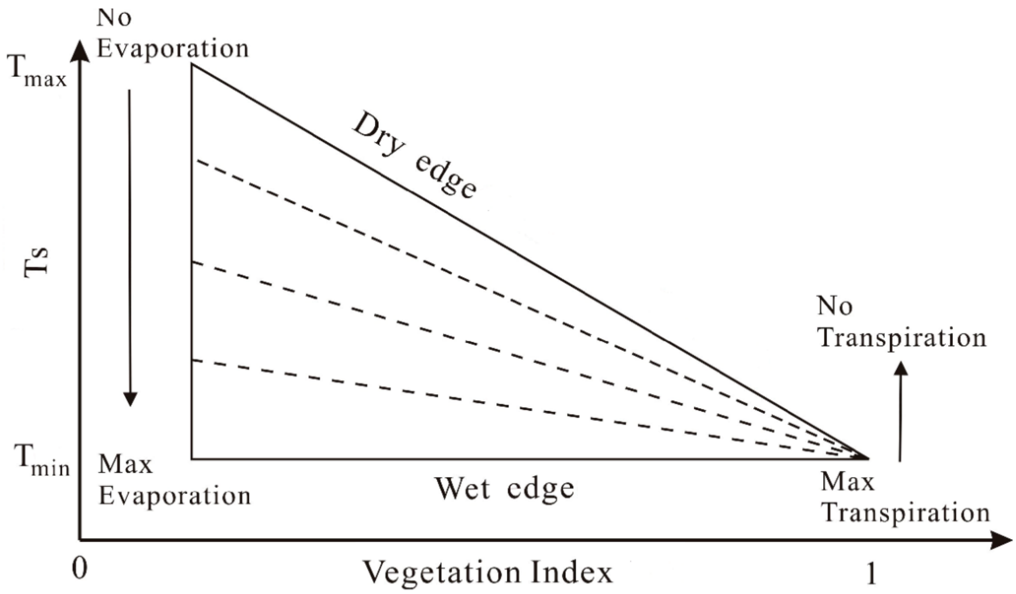

FIGURE 3. THE TS-VI FEATURE SPACE

Recent advances in optical remote sensing have allowed researchers to use different remote sensing products that reflect SM variability as ancillary information. A method based on "universal triangle" concept is used in several studies where a relationship between SM, vegetation index (VI) and surface radiant temperature (Ts) from optical remote sensing sensors is established. The universal triangle concept arises from the emergence of a triangular or trapezoidal shape when VI and Ts measures taken from heterogeneous areas are plotted in two-dimensional feature space – forming a Ts/VI scatterplot (Figure 3). Of the different land surface parameters, NDVI and LST are the most widely used. Theoretical and experimental studies have demonstrated the relationship between surface SM, NDVI and LST for a given region under specific climatic conditions and land surface types. This method is used by several studies to downscale microwave remote sensing retrievals of SM (Peng et al., 2017).

Three algorithms based on the triangle concept to improve the spatial resolution of the JASMIN product from 5 km to 1 km were investigated. The selected algorithms are applied using the thermal and optical infrared data from the MODIS instrument. The rationale for choosing these algorithms is: (a) they can be applied at a continental scale, (b) input data is readily available, and (c) they have been tested and documented over Australian regions. The study applied a step-by-step approach, where the algorithm identified as the simplest is implemented, tested and evaluated first, before moving to the next algorithm to explore skill that can be potentially be gained. In that respect, we started with the multiple linear regression method discussed in Piles et al (2011). To investigate whether the skill of the multiple linear regression method can be improved further by regularization, we employed the Least Absolute Shrinkage and Selection Operator (LASSO; Tibshirani, 1996) regression using the same feature variables used in the multiple linear regression method. Further, a more theoretically based method, in the form of "Disaggregation based on Physical And Theoretical scale Change" (DisPATCh; Merlin et al., 2012) was tested to identify any potential gain in the skill that could be achieved.

Downscaling methods

Multiple linear regression

The triangle concept has been used to develop a linking model that relates JASMIN SM data to MODIS derived NDVI and LST datasets. The linking model, in this case, is a multiple linear regression method which uses NDVI and LST data as the feature variables. Their relationship with SM can generally be expressed through a regression formula such as:

$$SM_{hres} = \sum_{i=0}^{n} \sum_{j=0}^{n} a_{ij} NDVI^{i} LST^{j} \qquad (11)$$

Piles et al. (2011) effectively used a second-order polynomial function to define the linking model between the LANDSAT surface radiant temperature/NDVI features and airborne SM estimates. The surface radiant temperature and NDVI were normalised to reduce the dependence of each parameter on ambient conditions. A similar approach was adopted here. However, the quadratic function used in our study was selected only after experimenting with linking models of various order, ranging from first to ninth order. We carried out these experiments over a test domain in south-eastern Australia, comprising the Murrumbidgee catchment, for the year 2010. The results were then compared against OzNet observations. It is found that the quadratic function provided the best estimate among all functions examined. The linking model used in the present study can be written as:

$$SM_{hres} = a_{00} + a_{01}T_n + a_{10}f_v + a_{11}T_n f_v + a_{02}T_n^2 + a_{20}f_v^2 \qquad (12)$$

Here, T_n stands for normalised LST (Eqn. 13) and f_v is the fractional vegetation cover defined as (Eqn. 14). T_n and f_v are calculated after masking cloud affected and land-water pixels from respective datasets.

$$T_n = \left[\frac{T_s - T_s^{min}}{T_s^{max} - T_s^{min}}\right]_{hres} \qquad (13)$$

$$f_v = \frac{NDVI - NDVI_{min}}{NDVI_{min} - NDVI_{max}} \qquad (14)$$

T_s^{max} and T_s^{min} are the maximum and minimum LST values for a day and region under study. Similarly, $NDVI_{max}$ and $NDVI_{min}$ are the maximum and minimum NDVI values for a day and region after masking the cloud and water pixels.

LASSO regression

The LASSO (Tibshirani, 1996) is an extension to the linear regression technique, where the regression coefficients are optimally reduced (shrinkage). In some cases, the regression coefficients are even reduced to zero, thereby ignoring a feature (selection). LASSO minimises the residual sum of squares as in classical linear regression, but the determination of regression coefficients is constrained by the sum of the absolute values of the coefficients being as small as possible. This is achieved by defining a regularization parameter (λ) in the cost function

(Eqn. 15) that determines the influence of the classical least square contribution (first term in the right-hand side of Eqn. 15) relative to the sum of modulus of the coefficients (second term on the right-hand side of Eqn. 15).

$$J(\beta_k) = \frac{1}{N}\sum_{n=1}^{N}(Y_n - \sum_k \beta_k X_{k,n})^2 + \lambda \sum_k |\beta_k| \tag{15}$$

The LASSO technique applied in the present study also uses normalised LST and NDVI features to derive the linking model. To estimate the optimal regularization parameter (λ), experiments were conducted on a training dataset covering south-east Australia, spanning the whole year of 2010. Based on the subjective evaluation and the objective verification against in-situ observations from OzNet network (results not shown for brevity), a value of 80 was selected for λ.

DisPATCh

The DisPATCh method is categorised as physically based as it links the land surface temperature data with surface SM through the soil evaporation process. The development of the DisPATCh method can be found in Merlin et al. (2005) and Merlin et al. (2008). The DisPATCh method in this study uses SEE concept to model the sub-pixel spatial variability of surface SM. The advantage of using SEE is that it is much more directly linked to remote sensing and a SEE model can be readily developed in conjunction with land surface temperature and surface SM. The disaggregation method in DisPATCh can be written as:

$$SM_{hres} = SM_{lres} + \left[\frac{\partial SM}{\partial SEE}\right]_{lres} . \left(SEE_{hres} - \overline{\langle SEE_{hres}\rangle_{lres}}\right) \tag{16}$$

SM_{hres} is the 1km downscaled SM, and SM_{lres} is the coarse-scale JASMIN SM. Here, we upscaled the JASMIN SM to 50 km resolution by averaging. This is to construct an accurate Ts-VI space, which is otherwise impossible in a 5 km resolution JASMIN grid, which encompasses only 25 MODIS LST pixels. From now on, coarse-scale JASMIN grid in DisPATCh refers to the 50 km resolution grid. SEE_{hres} is the MODIS-derived soil evaporative efficiency and $\overline{\langle SEE_{hres}\rangle_{lres}}$ it's average within a JASMIN grid. ∂SM/∂SEE is the partial derivative of SM to SEE evaluated at the coarser scale. Here, a linear model was used to define the sensitivity of SM to SEE, as this is found to be a good approximation at kilometre scales (Merlin et al., 2013).

MODIS derived SEE is expressed as a linear function of MODIS-derived soil temperature (T_s) and is given as:

$$SEE_{hres} = \left[\frac{T_{soil}^{max} - T_{soil}}{T_{soil}^{max} - T_{soil}^{min}}\right]_{hres} \tag{17}$$

T_{soil}^{max} and T_{soil}^{min} are the soil skin temperature at SEE=0 and SEE=1 respectively. The MODIS land surface temperature is linearly decomposed into soil temperature and vegetation temperature based on the Ts-VI feature space. The soil temperature is expressed as:

$$T_{soil} = \left[\frac{T_{LS} - f_r . T_v}{1 - f_r}\right]_{hres} \tag{18}$$

T_{LS} is the MODIS LST, f_r is the fractional vegetation and T_v is the vegetation temperature. The fractional vegetation cover is given as:

$$f_r = \frac{NDVI - NDVI_{soil}}{NDVI_{veg} - NDVI_{soil}} \tag{19}$$

$NDVI_{soil}$ is the NDVI corresponding to bare soil, and $NDVI_{veg}$ is the NDVI corresponding to full-cover vegetation. For the present study, $NDVI_{soil}$ and $NDVI_{veg}$ values are set to 0.10 and 0.80, respectively.

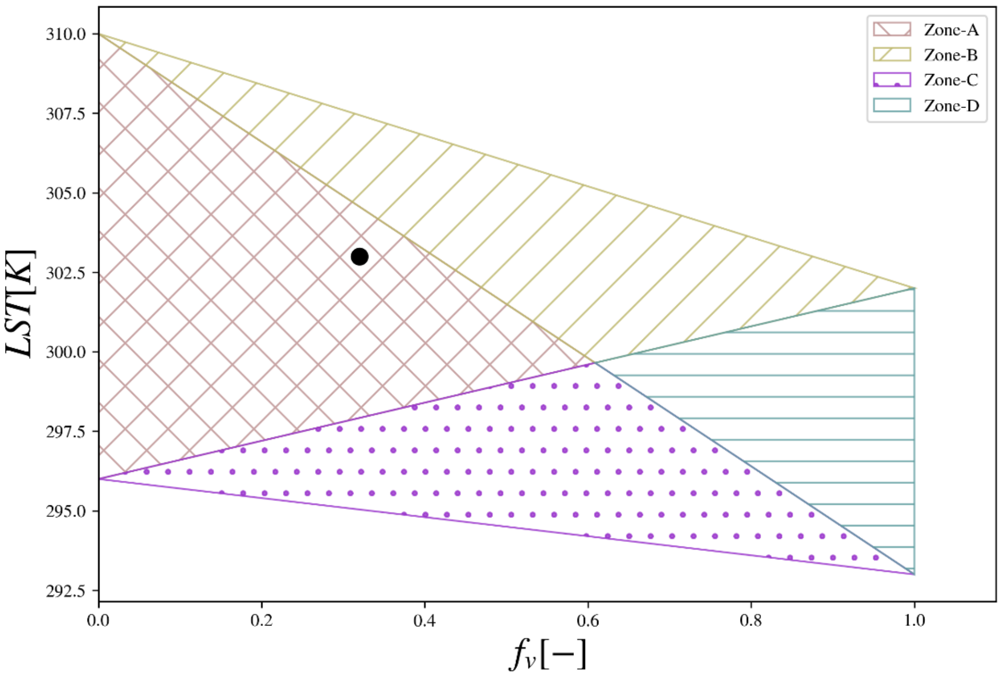

FIGURE 4. ESTIMATION OF VEGETATION TEMPERATURE USING THE "HOURGLASS" APPROACH. POLYGON DEFINED IN THE LAND SURFACE TEMPERATURE-FRACTIONAL VEGETATION COVER SPACE CONTAINS FOUR DISTINCT ZONES A, B, C, AND D. IN ZONE A (SOIL DOMINATED AREA), THE ESTIMATED VEGETATION TEMPERATURE IS CONSTANT, LEADING TO OPTIMAL SENSITIVITY OF ESTIMATED SOIL TEMPERATURE TO SURFACE SM. IN ZONE D, THE ESTIMATED SOIL TEMPERATURE IS CONSTANT WITH NO SENSITIVITY TO SURFACE SM. IN ZONE B AND C (MIXED SURFACE), THE SURFACE TEMPERATURE IS BOTH CONTROLLED BY SOIL EVAPORATION AND VEGETATION TRANSPIRATION WITH INTERMEDIATE (AVERAGE) SENSITIVITY OF ESTIMATED SOIL TEMPERATURE TO SURFACE SM.

The vegetation temperature was estimated using the "hourglass" approach described in Moran et al. (1994) and Merlin et al. (2012). By plotting the diagonals of the Ts-VI quadrilateral for each coarse-scale grid, four areas are distinguished in the feature space defined by surface temperature and fractional vegetation cover (Figure 2). In zone A, LST is mainly controlled by soil evaporation leading to optimal sensitivity of LST to surface SM. In zone D, LST is mainly controlled by vegetation transpiration with no sensitivity to surface SM. In zones B and C, LST is controlled by both soil evaporation and vegetation transpiration with intermediate sensitivity to surface SM. Based on this understanding, vegetation temperature was estimated for each zone as:

$$Zone\ A:\ T_v = \frac{T_v^{min} + T_v^{max}}{2} \tag{20}$$

$$Zone\ B:\ T_v = \frac{[T_v^{min}]_{SEE=0} + T_v^{max}}{2} \tag{21}$$

$$Zone\ C:\ T_v = \frac{T_v^{min} + [T_v^{max}]_{SEE=1}}{2} \tag{22}$$

$$Zone\ D\colon T_v = \frac{[T_v^{min}]_{SEE=0} + [T_v^{max}]_{SEE=1}}{2} \qquad (23)$$

F

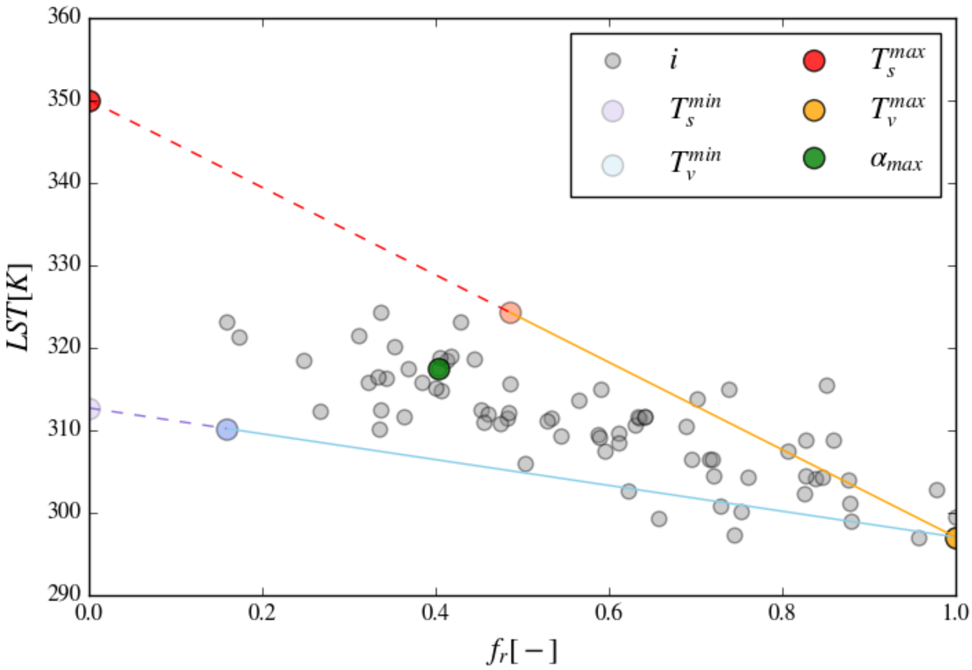

IGURE 5. ESTIMATION OF TEMPERATURE END MEMBERS. T_{soil}^{max}, T_{soil}^{min}, T_v^{min} AND T_v^{max} ARE ESTIMATED FROM THE SURFACE TEMPERATURE-FRACTIONAL VEGETATION COVER SPACE AND THE SURFACE TEMPERATURE-SURFACE ALBEDO SPACE WITHIN A GIVEN, UPSCALED JASMIN PIXEL. THE GREEN DOT REPRESENTS THE MODIS PIXEL WITH THE MAXIMUM ALBEDO. THIS PIXEL HAS A FRACTIONAL VEGETATION COVER LESS THAN 0.5, AND HENCE T_v^{max} IS SET TO T_v^{min}.

T_v^{min} and T_v^{max} being the vegetation temperature at the minimum and maximum water stress, respectively. End-members T_{soil}^{max}, T_{soil}^{min}, T_v^{min} and T_v^{max} are estimated at 1 km resolution by combining the spatial information provided by the LST-f_r and the LST-albedo feature space developed using the MODIS data within each coarser JASMIN grid point (Figure 3). Here, T_v^{min} is set to the minimum MODIS LST within each coarse-scale JASMIN grid. T_v^{max} is set to the LST of the MODIS pixel with the maximum albedo value (Figure 3). If $f_r < 0.5$ for the corresponding MODIS pixel, the vegetation T_v^{max} is set to T_v^{min}. The above condition is set to increase the robustness of the determination approach, particularly for the JASMIN grids where all surface conditions are not met. T_{soil}^{min} is calculated by extrapolating along the wet soil edge at $f_r = 0$. The wet soil edge is defined as the line passing through (SEE = 1, T_v^{min}) and through the data point such that all the data points with $f_r < 0.5$ are located above the wet soil edge (Figure 3). T_{soil}^{max} is estimated by extrapolating along the dry soil edge at $f_r = 0$. The dry soil edge is defined as the line passing through (SEE = 1, T_v^{max}) and through the data point such that all the data points with $f_r < 0.5$ are located below the dry soil edge.

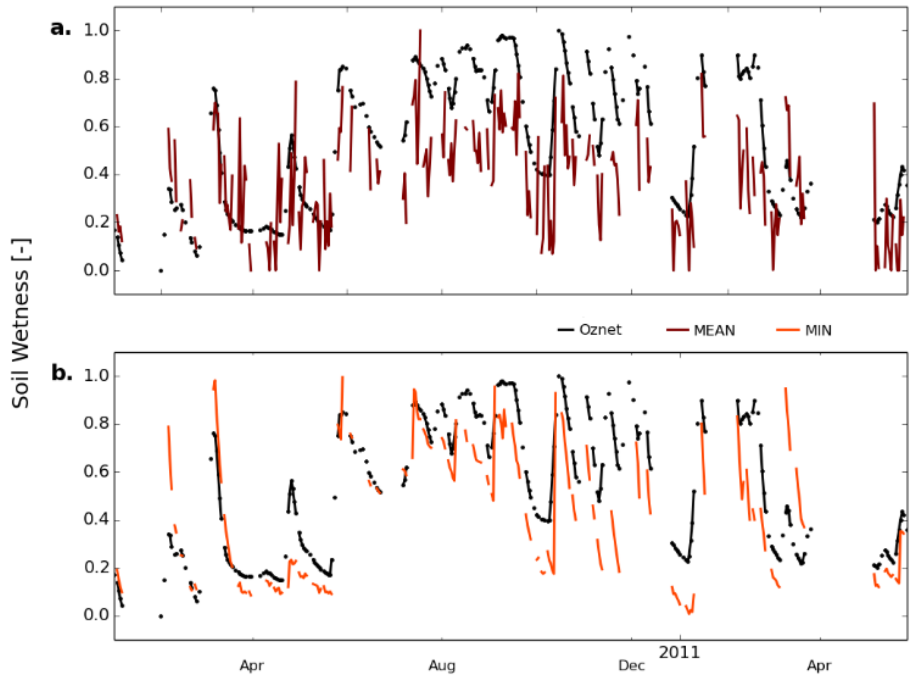

FIGURE 6. CALIBRATION OF DISPATCH SOIL PARAMETER. THE UPPER PANEL SHOWS THE COMPARISON OF IN-SITU SM (BLACK LINE) AGAINST DOWNSCALED SM OBTAINED BY APPLYING THE MEAN SOIL PARAMETER VALUE (BROWN LINE). THE LOWER PANEL DEPICTS THE SAME, EXCEPT THAT DOWNSCALED SM IS OBTAINED BY APPLYING THE MINIMUM SOIL PARAMETER VALUE.

A key factor in the performance of the DisPATCh algorithm is the correct calibration of the model depicting the relationship between SM and SEE. Here, a linear model was selected to estimate the SM sensitivity to SEE. This sensitivity is often referred to as SM parameter (SM_p) in DisPATCh literature. The model is calibrated from daily SEE and SM estimates at low resolution. In studies applying DisPATCh to disaggregate microwave SM retrievals, calibrated values of the SM_P were obtained by averaging estimates over multiple images collated over a few days (e.g.: Merlin et al., 2010). In the present study, daily sensitivity parameter is calculated using the MODIS and JASMIN datasets spanning the whole year of 2010. However, during the calibration phase, it was found that averaging of the daily SM_p led to large parameter values which introduced random errors in the downscaled SM, thereby reducing the temporal skill of the product. This is demonstrated through the comparison against ground observations from OzNet-Yanco site 9 (Figure 6a). Choosing the minimum parameter value rather than the mean is found to reduce these random errors (Figure 6b). Hence, in the present study, the calibrated parameter values are set to the minimum of SM_p values at each grid point from the 2010 time series.

EXPLORING THE LFMC-SM RELATIONSHIP

Live fuel moisture content is a key factor that contributes to the flammability of vegetation in ecosystems (Anderson, 1970, Yebra et al., 2018). Prediction of live fuel moisture content is inherently a very difficult problem since it is modulated by the complex physiological, phenological and ecological processes characteristic of the plant species. SM is one of the key variables that is known to influence plant water use. Recently, a new live fuel moisture content near-real-time product has been developed for Australia using a radiative transfer model inversion technique on the MODerate Resolution Imaging Spectroradiometer reflectance data (Yebra et al., 2018). This live fuel moisture content product forms the basis of the Australian Flammability Monitoring System (AFMS). The AFMS LFMC product has a temporal resolution of 4 days and a spatial resolution of 500m. The study brought together the AFMS-LFMC and JASMIN SM products to conduct preliminary research on the live fuel moisture content–soil moisture relationship on a national scale. This study also suggests an approach that may be constructive in advancing the ability to predict live fuel moisture content reliably to potentially support fire management applications.

Our approach was to first evaluate the relationship between the two variables at selected locations which sample the climatic zones and vegetation types typical of the Australian landscape. In that respect, we analysed the datasets over CosmOz, OzFlux and OzNet SM networks. Another reason to select these locations is the demonstrated skill of JASMIN at these sites (Vinodkumar and Dharssi, 2019). From our analysis, we identified that SMC from the 0-350 mm profile ($SMC_{0\text{-}350mm}$) provides the best skill in terms of the correlation with LFMC. The $SMC_{0\text{-}350mm}$ displays a strong relationship with the LFMC at different land cover types. One possible reason for this larger degree of agreement is that both the $SMC_{0\text{-}350mm}$ and LFMC exhibit strong seasonality. The deeper layers may not always display the strong seasonality exhibited by the shallower layers. Besides, the deeper layers may miss the short-term variations associated with individual weather events to which the plants and shallow soil profiles respond. Also, the upper and deeper soil layers can be disconnected in land surface models due to uncertainties in the parameterizations. This may result in deeper layers exhibiting little seasonality, rendering them less useful to predict seasonal LFMC changes.

The data used in the present study covers January 2010 to June 2020 period. To test the predictive model on the national scale adequately we reserve the data corresponding to the years 2012 and 2020 from the training dataset for validation purposes. The remaining data is used to construct the model.

LFMC predictive model

The study constructed a simple model for predicting LFMC using the gridded JASMIN SM product. We selected the 0-350 mm profile from JASMIN to model LFMC. The LFMC, in general, is influenced by a variety of factors other than SM availability, including plant physiology and ET (Qi et al. 2012). This possibly explains the somewhat different annual cycles exhibited by LFMC to $SMC_{0\text{-}350mm}$ (Figure 7). Hence, it is important to address some of these factors implicitly to derive a skilful model for LFMC based on SM. We adopt a modelling strategy similar to that discussed in Fovell et al. (2015), where it is hypothesised that LFMC departures from its annual cycle can be predicted with SM departures from its own annual cycle. Thus, the LFMC is predicted using a linear combination of an annual cycle model and a model to predict daily deviations from the annual cycle.

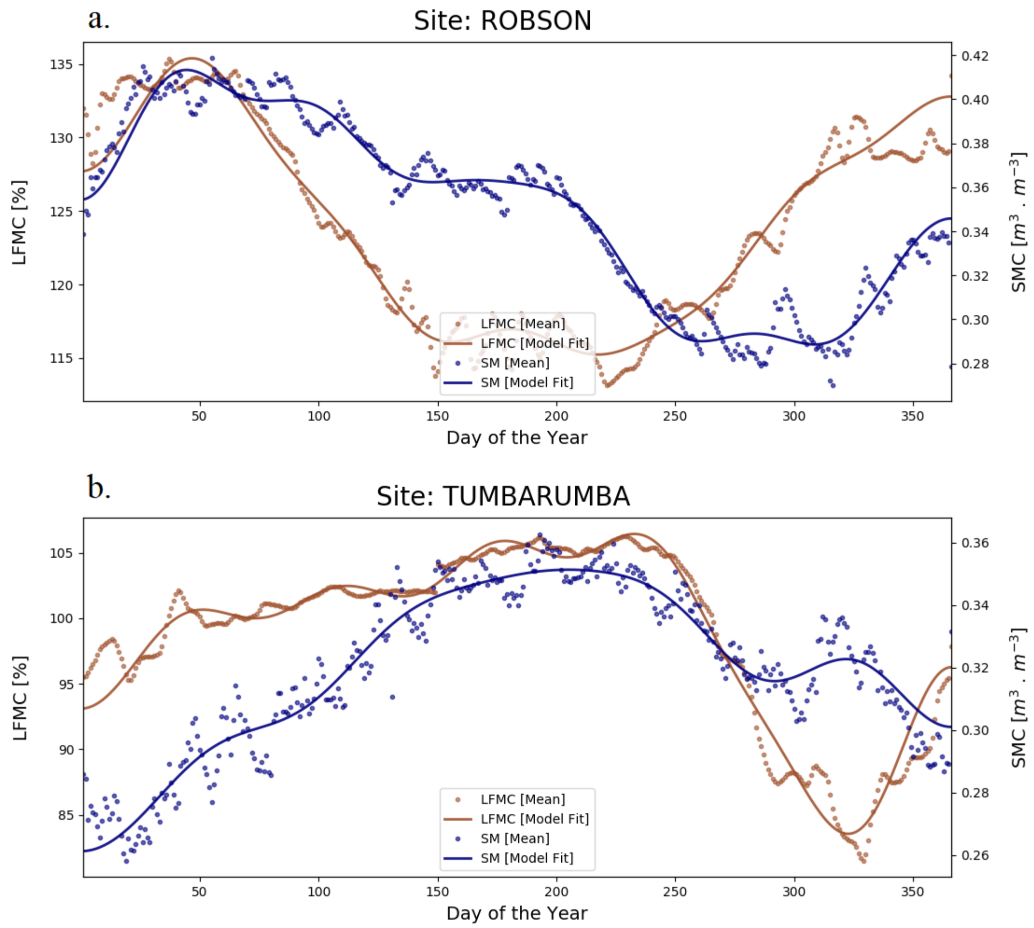

FIGURE 7. OBSERVED (DOTTED LINES) AND MODELLED (CONTINUOUS LINE) ANNUAL CYCLES OVER A) ROBSON CREEK, QUEENSLAND, AND B) TUMBARUMBA, NEW SOUTH WALES FOR LFMC (BROWN LINE) AND $SMC_{0\text{-}35CM}$ (BLUE LINE). THE ROBSON CREEK SITE IS LOCATED IN A TROPICAL RAINFOREST ECOSYSTEM IN THE NORTH-EASTERN QUEENSLAND AND THE TUMBARUMBA SITE IS LOCATED IN THE WET SCLEROPHYLL, BAGO STATE FOREST IN SOUTH-EASTERN NEW SOUTH WALES.

The LFMC data is about 10 times finer resolution than the JASMIN data. To develop the predictive model, the LFMC data is upscaled to 5 km resolution by taking an average of the LFMC values that are encompassed within each JASMIN pixel. The annual model for both LFMC and SM is based on a Fourier cosine series approximated to the 12^{th} harmonics, where day-of-the-year is used as the predictor variable. The daily deviation in LFMC from its annual cycle are computed using an ordinary least square regression model with the lagged, residual (deviation from the annual mean) SM as the independent variable. The predictive model can be written as:

$$LFMC = \alpha + \sum_{n=1}^{12} \beta_n \cos\left(n\frac{\pi D}{L}\right) + \gamma \acute{SM}_{lag} \qquad (24)$$

The 'a' term represents the intercept of both the Fourier series and the ordinary least square functions combined. 'β' is the slope of the ordinary least square model, D is the day of the year, L is the total number of days in a year (approximated to 366) and $\acute{SM}_{lag}$ is the lagged, daily SM deviations from its annual cycle. The model parameters change with location (grid points) except for the lag. A constant lag of 14 days is selected which helps to keep the predictive model simple without penalising the model skill.

The Fourier cosine series based annual cycle model (Equation 1) is found to be capable of estimating fairly odd-shaped annual cycles in both datasets, an example of which is shown in Figure 7 for the Robson tropical rainforest site (Figure

7a) and the Tumbarumba wet-sclerophyll site in New South Wales (Figure 7b). When the AFMS LFMC time series is compared to the annual model for the full data period, a sizable 51.8% of the reference series' variance is captured by the annual model, where the value represents the average for the 60 stations examined (see Supplementary Table 1). Similarly, for the $SMC_{0\text{-}35cm}$, the average variance that can be explained by the annual model is found to be 44.8%. The $SMC_{0\text{-}35cm}$ departures are generally found to have good agreement with the LFMC departures

The SM departures are generally found to have good agreement with the LFMC departures. This is illustrated in Figure 8, where a direct comparison is facilitated by superimposing the two residual time series over Baldry in New South Wales. However, it is readily apparent that there is a systematic phase difference between the two residual time series. A lag-correlation analysis for the residuals returned the highest correlation of 0.72 for a lag of 22 days over Baldry. This result further suggests that LFMC is responding directly and strongly to $SMC_{0\text{-}350mm}$ changes and the lag signifies the combined time taken for the rainfall received at the surface to percolate through the 0-350 mm layer and the subsequent water uptake process by the plant to occur. The lag between the two residual time series is found to vary from location to location. The mean (median) lag for grassland, woodland, forestland, and cropland are 14 (14), 15 (0), 10 (0) and 12 (16) respectively. The corresponding lag-correlation values are 0.65 (0.65), 0.42 (0.45), 0.27 (0.25), and 0.55 (0.56). The extremely short lag over a few of the forestland and woodland sites can be anomalous and may indicate a data representativeness issue. The noise in the data can possibly influence the accurate determination of the lag. It is found that the correlation does not vary significantly from one day to the next (not shown here for brevity).

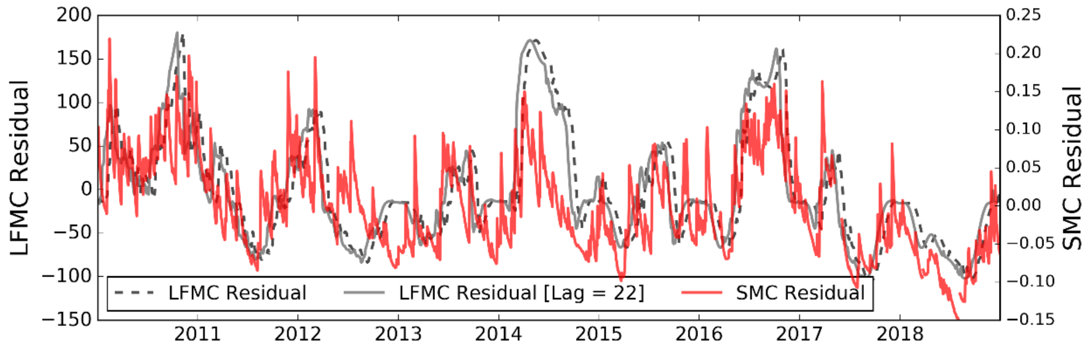

FIGURE 8. RESIDUAL TIME SERIES OF $SMC_{0\text{-}350MM}$ (RED LINE) AND LFMC (BLACK BROKEN LINE) BALDRY IN THE STATE OF NEW SOUTH WALES, AUSTRALIA (COORDINATES: 32.8710°S,148.5260°E). BALDRY SITE IS A MIX OF PASTURE AND REFORESTED WOODLAND. THE GREY SOLID LINE CORRESPONDING TO THE LFMC SHIFTED BACKWARD FOR 22 DAYS.

The site averaged (median) lag obtained was 13 (14) days. The daily departures of the 14-day lagged $SMC_{0\text{-}35cm}$ is found to provide a reasonable linear relationship with the LFMC residual time series at all locations and is hence selected to construct the model. The daily deviations in LFMC are thus predicted using that in 14-day lagged $SMC_{0\text{-}35cm}$, where the daily departures are calculated by removing the respective annual cycles from each dataset. A constant lag of 14-days helps to keep the predictive model simple. The annual cycle is calculated using the Fourier based model described above and in equation 24. Separate ordinary least square regression models with the residual 14-day lagged $SMC_{0\text{-}35cm}$ as the independent variable to predict daily changes in LFMC is developed for each location. The final predictive model is thus constructed using a linear combination of two sub-models - the Fourier series-based model to predict the annual cycle and the ordinary least square regression model to estimate the daily variations. As mentioned earlier, the model parameters are computed for each grid point due to the spatial variability in LFMC and SM.

FINDINGS

DEVELOPMENT AND VALIDATION OF JASMIN SYSTEM

There is evidence that KBDI and SDI perform poorly in predicting near-surface SM (Vinodkumar and Dharssi, 2017; Holgate et al., 2017). This is critical from a fire prediction standpoint, given the relationship between moisture states in forest litter and surface soil (Hatton et al. 1988). SM from land surface models within a numerical weather prediction system can provide more accurate estimates than that from the above indices (Vinodkumar et al., 2017). In Australia, the SM analyses from operational NWP systems run by the Bureau of Meteorology are coarse in resolution (~ 18 km), and the skill can be limited by large uncertainties that exist in NWP forcing - especially precipitation. Hence, JASMIN, a prototype, high resolution, offline land surface modelling system has been developed by the Bureau of Meteorology (Dharssi and Vinodkumar, 2017).

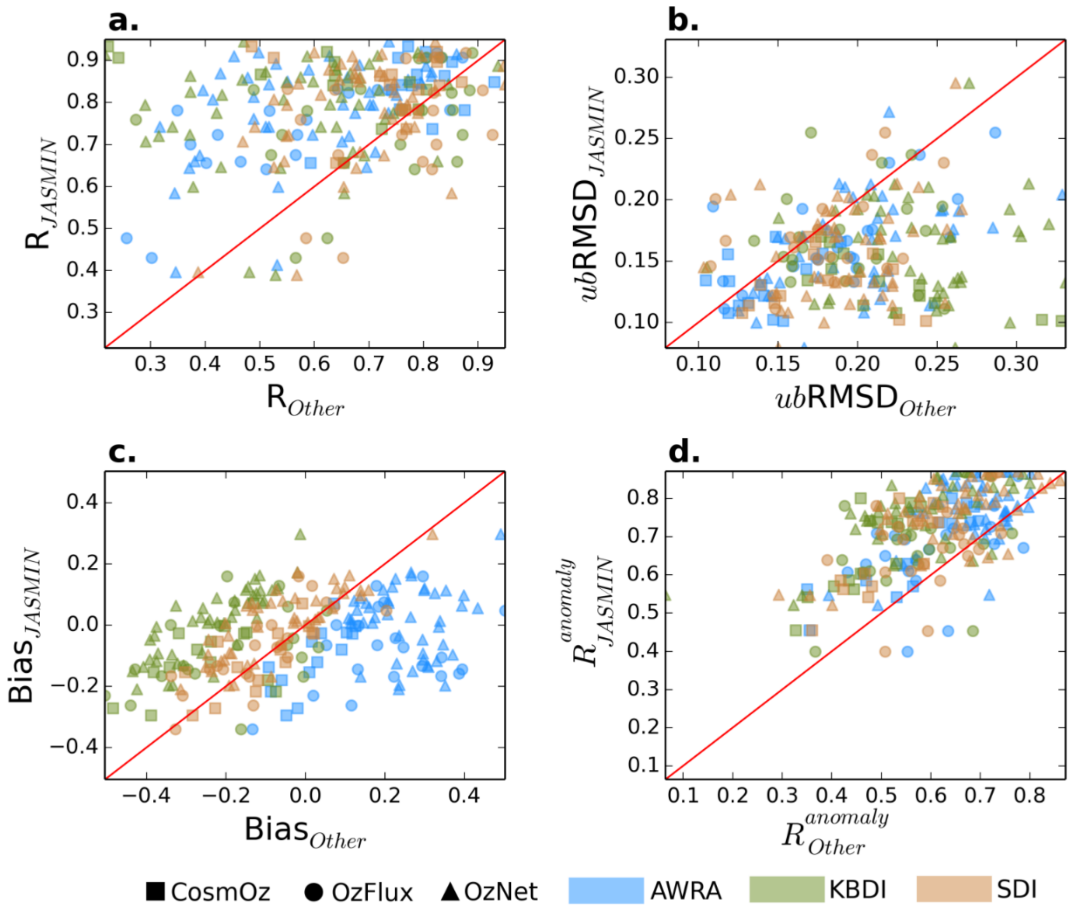

FIGURE 9. SCATTER PLOTS DEPICTING A) CORRELATION, B) UNBIASED RMSD, C) BIAS AND D) ANOMALY CORRELATION. THE Y-AXIS SHOWS THE SKILL SCORES OF JASMIN SOIL WETNESS AGAINST IN-SITU OBSERVATION. THE X-AXIS CORRESPONDS TO THE SKILL SCORES OF THE OTHER THREE MODELS (AWRA-L, KBDI AND SDI) AGAINST IN-SITU OBSERVATIONS. EACH COLOUR REPRESENTS A MODEL TYPE DEPICTED ON THE X-AXIS (I.E., AWRA, KBDI AND SDI). EACH SYMBOL REPRESENTS AN OBSERVATION NETWORK TYPE. THE RED LINE IS FOR MERE REFERENCE.

A systematic validation of JASMIN using in-situ data was conducted to support the development and utilization of JASMIN for application in operational fire prediction and risk management practices in Australia. The need for a spatially and temporally extensive ground-truthing of JASMIN is addressed by using three large-scale SM networks. This study also complements the traditional ground-truthing methodologies with a relatively new validation technique called extended triple collocation (results not shown). The study also utilised SM from AWRA-L version 5.0 (Frost et al., 2016), KBDI and SDI models for comparison and benchmarking. The AWRA-L model has since been updated to version 6.0 with improvements to model structure and physics (Frost et al., 2018). The JASMIN SM used in the present study is valid at 00 UTC. All spatial data collocation to in-situ locations is done using the nearest neighbour method. KBDI and SDI values are converted to SMC by subtracting the values from their respective maximum. To enable a fair comparison, all SM products and indices are converted to soil wetness (normalised between [0, 1]) using their maximum and minimum values from respective long time series. Such normalization has been done by many other SM verification studies (e.g., Brocca et al., 2011). However, this rescaling approach is sensitive to outliers in observations and hence a careful visual inspection is performed to remove any erroneous measurements.

Figure 9 represents the skill scores of JASMIN plotted against that of the other three models (i.e., AWRA-L, KBDI and SDI) for shallow layer observations from the three ground-based networks. The skill scores presented are correlations (Figure 9a), ubRMSD (Figure 9b), bias (Figure 9c) and anomaly correlations (Figure 9d). JASMIN generally exhibits a stronger correlation compared to the other three models (Figure 9a). This is especially true over CosmOz and OzNet networks. The median correlation for JASMIN obtained against CosmOz, OzNet and OzFlux are 0.85, 0.81 and 0.78 respectively (Table 1). JASMIN consistently displays a strong positive correlation over CosmOz sites where $R > 0.60$ at all sites. Out of the total 45 sites in OzNet network, JASMIN displays $R > 0.60$ for all except 4 sites. For OzFlux, JASMIN captures the temporal patterns well for 19 sites out of 21, with $R > 0.60$ at all these sites. Only Warra (0.43) and Samford (0.48) exhibit a weak correlation ($R < 0.6$). AWRA-L and KBDI exhibit a larger scatter in correlations compared to SDI. Most of the poor temporal correlations exhibited by AWRA-L are over the OzNet and OzFlux sites. We use the top 0 – 0.1 m soil profile from AWRA-L for comparison against OzNet & OzFlux. The poor performance of AWRA-L in capturing shallow SM dynamics may be due to the fact the surface energy balance terms in the AWRA-L are simplified when compared to JULES LSM. AWRA-L is specifically designed and calibrated to capture runoff dynamics (Frost et al., 2015). AWRA-L over CosmOz sites performs better compared to the other two networks. This is because AWRA-L 0 – 1 m profile was used for verification against CosmOz. It is noted that the AWRA-L 0 – 1 m profile agrees better with CosmOz observations compared to the 0 - 0.1 m profile (not shown). We chose the deeper profile from AWRA-L since the CosmOz observational depths are usually greater than 0.1 m. KBDI shows a relatively better performance over OzFlux compared to OzNet and CosmOz. A majority of OzFlux sites are situated in high rainfall regions, and some among them are in the tropics. KBDI is known to perform well in regions with a warm climate and higher annual rainfall totals (Spano et al., 2006). This is typical of the region (south-eastern US) for which KBDI was designed and calibrated.

Network	CosmOz				OzFlux				OzNet			
Model	*R*	*Bias*	*ubRMSD*	R_{an}	*R*	*Bias*	*ubRMSD*	R_{an}	*R*	*Bias*	*ubRMSD*	R_{an}
AWRA-L	0.78	**0.02**	0.14	0.59	0.57	0.20	0.20	0.57	0.60	0.27	0.20	0.70
JASMIN	**0.85**	-0.10	**0.13**	**0.68**	0.78	**-0.07**	**0.16**	**0.68**	**0.81**	**0.02**	**0.17**	**0.78**
KBDI	0.65	-0.24	0.21	0.47	0.78	-0.18	0.19	0.56	0.59	-0.23	0.25	0.61
SDI	0.77	-0.09	0.17	0.55	**0.79**	-0.12	0.18	0.62	0.68	-0.07	0.19	0.67

TABLE 1. THE MEDIA SKILL SCORES FOR EACH MODEL ACROSS THE THREE OBSERVATION NETWORKS. THE BEST SCORE FOR EACH NETWROK IS GIVEN AS BOLD NUMBERS.

The lower ubRMSD in JASMIN compared to the other three models is represented by the general clustering of points below the reference line in the respective scatter plot (Figure 9b). This indicates that the amplitude of short-term variations in observed soil wetness is well captured by JASMIN compared to the other three models. The poor ubRMSD scores generally correspond to sites with poor temporal correlations in all models. The closer agreement of JASMIN to observe amplitudes are reflected by the lowest median scores of ubRMSD across all networks (Table 1). KBDI generally show large deviations from observation (Figure 9b). KBDI has the largest median ubRMSD values for CosmOz and OzNet networks (Table 1). However, for OzFlux, AWRA-L has the lowest skill in terms of ubRMSD (0.20) closely followed by KBDI (0.19).

AWRA-L generally has a large dry bias in the simulated surface layer soil wetness compared to observations. This is evident in their comparisons over OzFlux and OzNet observation networks (Table 1). This is also highlighted in the scatter plots (Figure 9c). KBDI, in general, show a wet bias. This is reported in earlier studies as well (Vinodkumar et al., 2017). KBDI models ET as an inverse natural exponential function of mean annual rainfall in the denominator. This leads to lower ET rates in regions of smaller annual rainfall totals. These lower ET rates are found to introduce wet bias in SM simulated by KBDI. SDI also shows a wet bias, but relatively small compared to KBDI. SDI biases are comparable to that in JASMIN (Figure 9c). The assumption of ET as a linear regression function of maximum temperature in SDI may have helped to reduce the wet bias seen in KBDI, on which it is based (Finkele et al., 2006).

The anomaly correlations for each model to observations from three networks are shown in Figure 9d. The ability of the model to capture the short-term fluctuations in observations is quantified by the anomaly correlation metric. The moisture fluctuations in the shallow soil layer are influenced by weather events and radiative forcing. It is worth noting here that all models considered in the present study are driven by the same precipitation analysis (AWAP). Hence the difference in fluctuations characterised by each model cannot be due to the difference in rainfall amounts for a particular event in the driving data. These differences, however, can be due to how each model represents surface energy and water balance processes. JASMIN is found to have a relatively higher anomaly correlation when compared to AWRA-L, KBDI and SDI (Table 1). Given the complexity of physical processes that govern surface SM dynamics, these results indicate a robust modelling approach in JULES LSM. The governing complex physical processes also explain the low skill in KBDI and SDI. For example, both of these models do not consider the majority of physical factors like soil type, vegetation type, or terrain aspect which affect SM. Further, no information on atmospheric controls of ET like net radiation, wind speed, relative humidity is used.

The comparison of the new JASMIN system against the current operational KBDI and SDI methods through verification against in-situ SM observations reveals some encouraging results. JASMIN has better skill than KBDI and SDI models in capturing the high-frequency moisture fluctuations observed in the shallow soil layer. The high skill of JASMIN is maintained over different land use/land cover classes, two geographic zones (tropics and extra-tropics), and also during dry and wet seasons. Since the moisture fluctuations in both litter and shallow soil layer are influenced by weather events and radiative forcing, the shallow soil layer can be considered as a good representation of the litter layer. Having a good skill in simulating shallow soil layer wetness is critical as it is suggested that during spring, moisture at the surface and extreme upper layer largely determines the condition of the available forest fuels. The modest representation of litter layer SM in KBDI and SDI partly reflects the limitation of empirical ET estimation methods in them. These formulations are designed and calibrated for a particular region and cannot be applied for a vast landmass like Australia whose climate significantly vary in space. The lack of information on atmospheric controls of ET, like net radiation, wind speed, relative humidity may introduce errors, particularly biases in the estimates of these models.

CALIBRATION OF JASMIN

The calibration exercise was conducted to illustrate the effective adoption of JASMIN in current operational practices by applying simple calibration methods. We apply the calibration methodology to convert native JASMIN SMC available in kg m^{-2} to SM deficit values specified in a range between 0–200 mm, as required by FFDI. The calibration offers a simple, faster, and cost-effective way to make significant upgrades to the existing operational systems used by fire and other environmental agencies. The calibration methods applied here are minimum-maximum matching, mean-variance matching and cumulative distribution function matching. The calibrated products are evaluated against observations using Pearson's product-moment correlation and extended triple collocation methods (Vinodkumar and Dharssi, 2019). A qualitative evaluation of the traditional indices and JASMIN rescaled products against Moderate resolution Imaging Spectro-radiometer (MODIS) fire radiative power (FRP) data is also carried out.

Pearson's correlation analysis

In situ network	Correlation					Anomaly correlation				
	KBDI	*MM*	$\mu - \sigma$	*sCDF*	*tCDF*	*KBDI*	*MM*	$\mu - \sigma$	*sCDF*	*tCDF*
0-350 mm profile										
CosmOz (surface)	-0.69	-0.84	-0.82	-0.76	-0.79	-0.47	-0.66	-0.61	-0.50	-0.59
OzFlux (surface)	-0.75	-0.80	-0.80	-0.73	-0.79	-0.58	-0.70	-0.68	-0.57	-0.66
OzFlux (root zone)	-0.86	-0.85	-0.85	-0.78	-0.85	-0.65	-0.63	-0.63	-0.49	-0.62
0-1 m profile										
CosmOz (surface)	-0.69	-0.73	-0.70	-0.65	-0.67	-0.47	-0.57	-0.55	-0.48	-0.54
OzFlux (surface)	-0.75	-0.74	-0.73	-0.60	-0.71	-0.58	-0.64	-0.61	-0.51	-0.60
OzFlux (root zone)	-0.86	-0.82	-0.82	-0.65	-0.82	-0.65	-0.63	-0.62	-0.48	-0.60

TABLE 2. PEARSON'S PRODUCT-MOMENT CORRELATIONS OF KBDI AND JASMIN BASED SMD PRODUCTS AGAINST IN-SITU SM OBSERVATIONS. THE VALUES REPRESENT A NETWORK AVERAGE.

Pearson's product-moment correlation against in situ SM observations. The period of verification is 4 years, from 2012 – 2015. Measurements used here comprise 21 sites from OzFlux network and 11 from CosmOz network. Only sites with at least a year of valid data are selected for calculating correlations. Scores are only presented for sites with significant correlation with p-values < 0.001. For the sake of brevity, only results corresponding to KBDI are presented.

Table 2 depicts the Pearson's product-moment correlation for KBDI and corresponding four rescaled JASMIN products from both 0 – 350 mm and 0 – 1 m model soil profiles. The values represent a network average. The negative values indicate that the model fields are in deficit form whereas observations are given as SMCs. For the CosmOz network, the highest correlations for both full (-0.84) and anomaly (-0.66) time series are obtained for MM product based on 0 – 350 mm model soil profile. KBDI correlations against CosmOz for full and anomaly time series are -0.69 and -0.47 respectively. The correlations of JASMIN products decrease when the 0 – 1 m soil profile is used. This is because CosmOz observations represent shallow layer SM where observation depths are usually below 400 mm. The comparison of JASMIN product rescaled to KBDI and OzFlux surface and root zone observations also indicate that the rescaling is done on JASMIN product from the 0 – 350 mm profile in general yield a higher correlation than that from a 1 m profile. About 42% of the deep layer observations in OzFlux have probes located at 500 mm. Only 16% of total sites have probes located at 1 m. This possibly made the 0 – 350 mm model profile more representative of observations than the 1 m profile. The highest correlation against OzFlux surface observations is -0.80 and are obtained for both MM and μ-σ methods which use 0 – 350 mm soil profile. The largest anomaly correlation of -0.70 is also obtained for the MM method. For OzFlux root-zone observations, MM matching method and μ-σ methods that use the 0 – 350 mm model profile deliver the highest correlation for both full (-0.85) anomaly time series (-0.63).

Correlations for both full and anomaly time series from all JASMIN products, except *s*CDF, are generally higher than that of KBDI. The MM, μ-σ and tCDF methods give similar correlations for all observation networks. Since MM and μ-σ matching are effectively linear transformation methods, they both preserve the correlations in the original data and hence provide similar results. The tCDF matching technique is a non-linear method and corrects the mismatch in seasonality, statistical mode between KBDI and the JASMIN product. This may cause JASMIN to lose some of the skill over sites where KBDI does not perform well. This is possibly reflected in the comparison against CosmOz where tCDF has a lower correlation than MM and μ-σ methods. The improved skill of tCDF in root zone also underlines this as KBDI has a good temporal correlation with observations. The tCDF matching consistently gives a higher correlation than the *s*CDF matching technique. It is noted that the *s*CDF matching introduces noise in the rescaled outputs, possibly arising from lack of sufficient spatial samples from a single day to characterise the complete dynamic range of two products.

Evaluation against fire radiative power data

Following Holmes et al (2016), a subjective evaluation of soil dryness products against Moderate resolution Imaging Spectro-radiometer (MODIS) fire radiative power (FRP) data are presented in this section. FRP estimates are available with every active fire pixel reported in the MOD14 and MYD14 fire products derived from the MODIS instrument onboard Terra and Aqua satellites (Giglio et al., 2003). The MODIS FRP retrieval is based on the relationship between the emitted fire energy and infrared brightness temperature estimates in the 4 μm region (Kaufman et al., 1998). The algorithm is valid for FRP retrievals of fires with flaming temperatures greater than 600 K and occupying a pixel fraction less than 0.1 (Wooster et al., 2003). The FRP is given in a unit of megawatts (MW) per pixel.

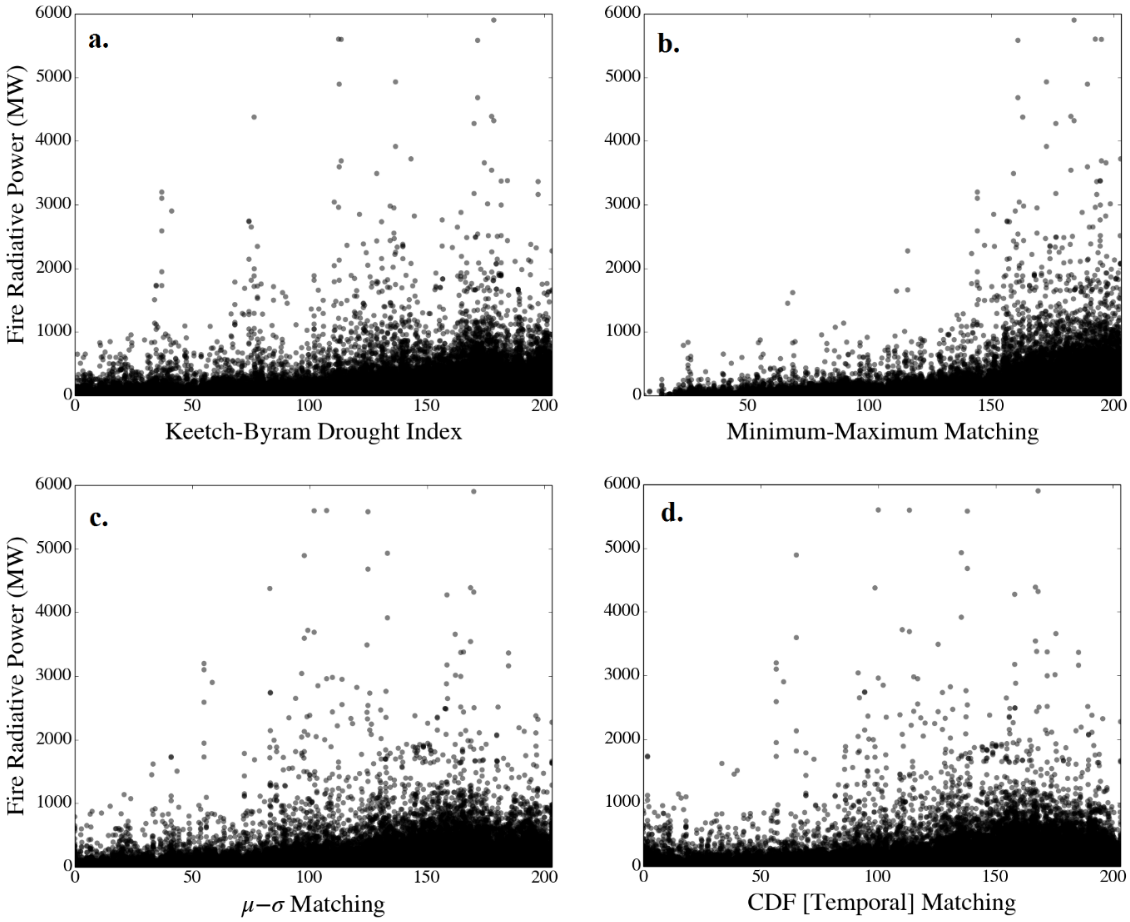

FIGURE 10. SCATTER PLOT DEPICTING MODIS FRP PRODUCT AGAINST A) KBDI, JASMIN RESCALED USING B) MM METHOD, C) M–Σ METHOD AND, D) TEMPORAL CDF MATCHING METHOD. JASMIN PRODUCTS CORRESPOND TO 0.35 M MODEL SOIL PROFILE. THE DATASETS SPAN FROM JANUARY 2012 TO FEBRUARY 2013 AND COVERT THE WHOLE OF AUSTRALIA.

Figure 10 depict scatter plots of MODIS FRP against KBDI and JASMIN products rescaled to KBDI using various methods. The KBDI display wet soils with dryness values < 100 mm for some fires with intensity > 2000 MW. The shift towards a drier soil in JASMIN MM rescaled product (Figure 10b) makes these large intensity fires attributable to higher SMDs. Results from the scatter plot for the μ–σ method (figure 10c) are quite different from those of the MM method. Most of the high-intensity fires in μ–σ method occur at SMD values between 50 – 180. This is also true for JASMIN product rescaled using both spatial (not shown for brevity) and temporal CDF matching (Figure 10d).

One of the advantages of using the μ-σ and tCDF techniques is that they preserve the climatology of the traditional SMD data. The differences are then, mainly due to random variations. This may be critical for some users, who already have their systems tuned towards the climatology of KBDI or SDI. It is not known whether the FFDI calculations are tuned to offset the bias in the traditional indices. Hence, it may be that the usability of these new datasets is solely reliant on improvement to correlations and not to other factors such as bias. In that case, MM and μ-σ methods present the best possible options. Temporal correlations in the raw JASMIN dataset are preserved in these two methods due to the linear nature of transformations. Otherwise, the errors from each rescaling method may become important and an accurate estimation of errors can conceivably contribute to a more realistic and reliable FFDI.

The similarity in scatter plots of KBDI and the corresponding μ–σ and tCDF products underline the similar seasonality in these datasets. The shift towards a drier soil in the MM method produces a scenario where FRP increases somewhat exponentially with SMD. The large FRP values now coincide with drier soils in the MM method. Holmes et al. (2016) using a SM proxy noted that the large MODIS FRP values coincide with very dry soils. The scatter plot of the original indices shows that higher FRP values occur over wet soils as well as dry soils. Generally, large intense fires are associated with sufficiently dry live fuels and larger dead fuels. The drying of these large fuel loads is associated with prolonged drought and hence large SMD. In that respect, it could be argued that the drier soils in the MM method corresponding to large FRP values present a more realistic scenario. This drier soil m in the MM method also results in elevated FFDI values.

DOWNSCALING OF JASMIN

The downscaling study explored the applicability of some of the universal triangle concept-based methods to downscale JASMIN SM from 5 km to 1 km spatial resolution. Specifically, the multiple linear regression method discussed in Piles et al. (2011) and the DisPATCh method discussed in Molero et al. (2016) were implemented and evaluated. The main reason for selecting these methods was that they have been tested and documented to derive SM information at 1 km spatial resolution over Australian regions. Further, the input data used in these methods are readily available. To investigate whether the skill of the multiple linear regression method can be improved further by regularization, we implemented the LASSO regression using the same feature variables used in the multiple linear regression method. The downscaling algorithms are only applied to the top JASMIN soil layer (0-100 mm). One of the main factors controlling the shape of Ts-VI scatter is the surface SM. Studies have shown that the combined use of optical and thermal infrared data can be used to derive moisture estimates for the top 50 mm soil layer (e.g., Sandholt et al., 2002, Stisen et al., 2008). Even though there is a mismatch in scales regarding the soil column each method represents, the topmost soil layer in JASMIN is a good approximation to that the Ts-VI method represents.

Results from the downscaling methodologies indicate that it is feasible to improve the spatial resolution of JASMIN using all three disaggregating algorithms and preserve the general large-scale spatial structure seen in JASMIN SM estimates (Figure 11). However, the seasonal means obtained at 1 km shows that each product displays characteristic SM spatial variability at fine scales. Results from the comparison with ground-based SM measurements indicate that there is no significant degradation of the bias in the three methods when moving to higher spatial resolution (Figure 12). However, the regression methods degrade the temporal correlations and the ubRMSD scores. The DisPATCh method produces the best skill among the three algorithms tested here, and the skill scores from DisPATCh are comparable to those of the original JASMIN time series.

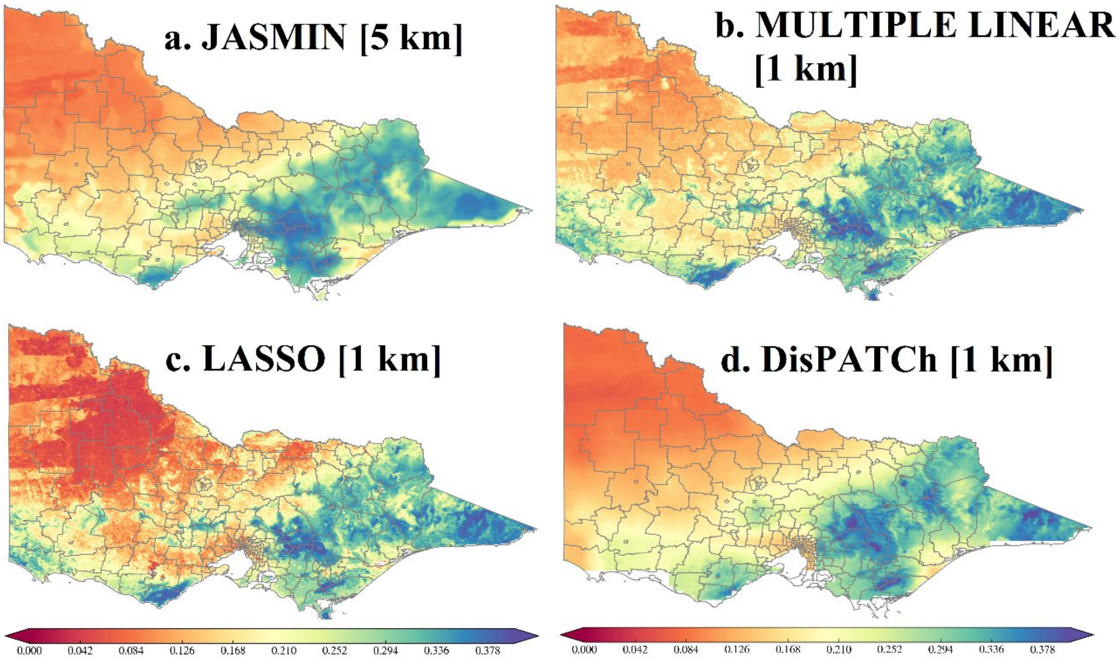

FIGURE 11. SEASONAL AVERAGE VOLUMETRIC SM FOR SOUTHERN-HEMISPHERE AUTUMN (MARCH – APRIL) FROM (A) JASMIN AT 5 KM RESOLUTION, (B) MULTIPLE LINEAR REGRESSION METHOD AT 1 KM, (C) LASSO REGRESSION METHOD AT 1 KM RESOLUTION, AND (D) DISPATCH AT 1 KM RESOLUTION.

The low skill observed in regression methods possibly resulted from the large random errors attributable to the methods or uncertainties in the feature variables. It is worth noting that even the minimum and maximum limits applied to calculate the normalised LST and NDVI datasets (feature variables in the regression method) can introduce uncertainties in the downscaled SM output. Further research is required to identify and minimise some of the uncertainties associated with both MODIS LST and NDVI datasets and to provide robust quality control.

Uncertainties in the MODIS input datasets have an important influence on the DisPATCh results as well, in addition to the uncertainties arising from the model assumptions and calibrations. It is found that calibration has a significant influence on the DisPATCh model behaviour. Further research is needed to calibrate the model so that the spatial variability in SM is accurately captured. One aspect of DisPATCh that needs to be revisited is the modelling of SM sensitivity to the soil evaporative efficiency. The model in the present study was chosen for its simplicity and its ability to represent the general behaviour of soil evaporative efficiency over the full range of SM. However, studies have shown that the SM sensitivity to soil evaporative efficiency can be non-linear and influenced by various factors including atmospheric demand, soil texture etc. It is important to note that the DisPATCh algorithm is evolving and will continue to do so. Further work is required to test and evaluate the new ideas that will be developed concerning DisPATCh and will be a focus of future research.

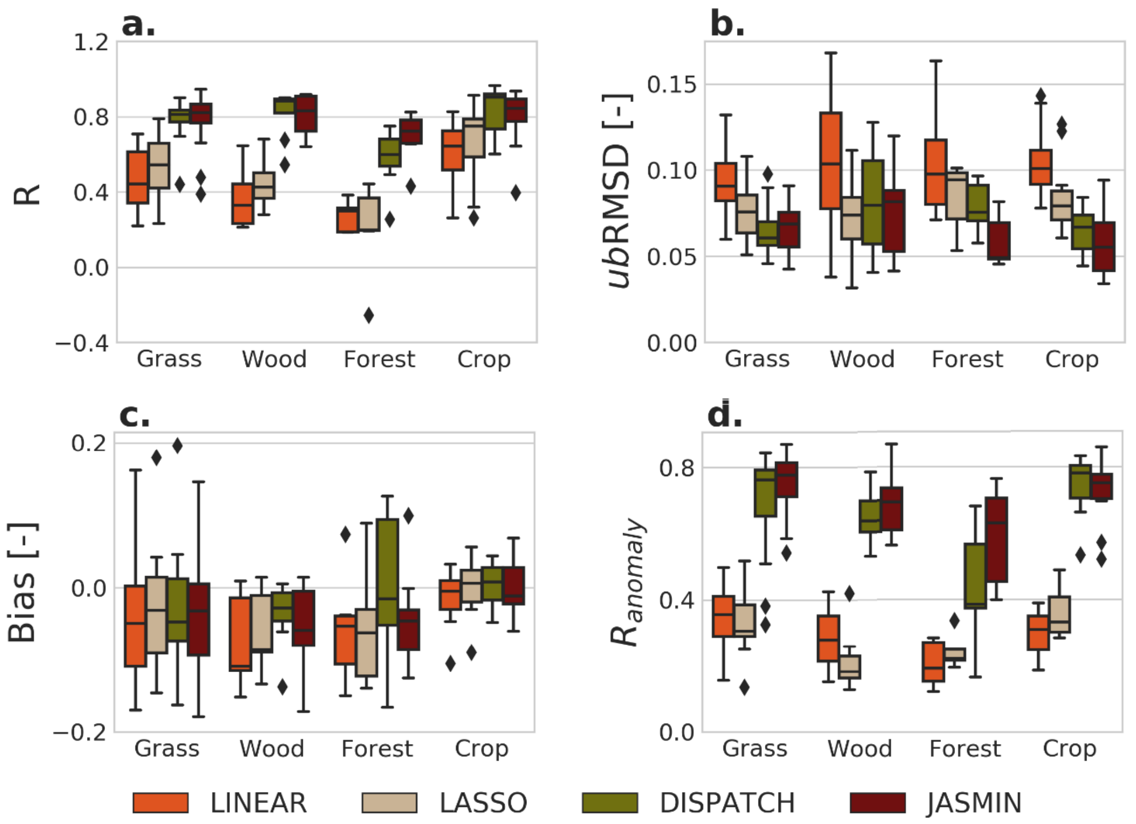

FIGURE 12. THE SKILL OF SM PRODUCTS OVER VARIOUS LAND COVER TYPES: A) PEARSON'S CORRELATION, B) UNBIASED RMSD, C) BIAS, AND D) ANOMALY CORRELATION. THE GROUPING IS DONE BASED ON THE LAND COVER TYPE OF THE OBSERVING SITE. THE OUTLIERS ARE MARKED AS DIAMONDS. THE ORANGE BOXES REPRESENT MULTIPLE LINEAR REGRESSION METHOD, LIGHT KHAKI COLOUR REPRESENTS LASSO METHOD, THE GREEN BOXES REPRESENT DISPATCH AND THE MAGENTA COLOURED BOXES REPRESENT THE ORIGINAL JASMIN PRODUCT AT 5 KM RESOLUTION.

EXPLORING LFMC-SM RELATIONSHIP

In this component of the project, we explored the relationship between live fuel moisture content and SMC on a national scale. The two variables represent landscape dryness at different strata and the latter can be a good indicator of the former (Fovell et al., 2015, Qi et al., 2012). Remote sensing techniques now allow sampling LFMC at a continental scale more regularly, which is impractical using the traditional, manual methods. However, temporal, and spatial gaps in remote sensing data exist, mainly due to satellite return time and cloud cover. Further, as mentioned earlier, a critical gap exists in predicting the moisture status of live fuels over periods of weeks to seasons. Our study is a first step towards addressing the limitations of remote sensing techniques in estimating LFMC and developing a predictive model that can be incorporated into future operational applications. The study made use of readily available gridded LFMC and SM products from the AFMS and JASMIN systems to identify the functional relationship between SM and LFMC.

Our approach is to first evaluate the relationship between the two variables at selected locations which sample the climatic zones and vegetation types typical of the Australian landscape. In that respect, we analyse the datasets over CosmOz, OzFlux and OzNet. A lag-correlation analysis is conducted between LFMC and SM from all the native JASMIN layers and the combination of layers that can be rationally derived using the four native soil profiles. The results presented in Figure 13 depicts the maximum lag-correlation and the corresponding lag (in days) for each site. The skill scores are segregated into four broad land cover types. The land cover classification is made based on the information from *in-situ* locations. The results indicate that the strength of the relationship between LFMC and SM varies from site to site. The observed variation in the correlation can be caused by a variety of factors, including spatial variability in plant type, physiology and morphology, climate, soil properties and depth. The range in lag time indicates that there is a significant difference in the physical processes happening at each location, from the transport of water through the soil from the surface to the root-zone and the eventual uptake of moisture by plants.

The study aims to develop a simple model to explain the relationship between LFMC and SM. In that respect, we prefer to use a single SM profile as the predictor for LFMC. From our analysis, we identify that SMC from the 0-350 mm profile ($SMC_{0\text{-}350mm}$) provides the best skill in terms of the correlation with LFMC. The $SMC_{0\text{-}350mm}$ displays a strong relationship with the LFMC at different land cover types. One possible reason for this larger degree of agreement is that both the $SMC_{0\text{-}350mm}$ and LFMC exhibit strong seasonality. The deeper layers may not always display the strong seasonality exhibited by the shallower layers. Besides, the deeper layers may miss the short-term variations associated with individual weather events to which the plants and shallow soil profiles respond. Also, the upper and deeper soil layers can be disconnected in land surface models due to uncertainties in the parameterizations. This may result in deeper layers exhibiting little seasonality, rendering them less useful to predict seasonal LFMC changes. This also gives rise to artificial correlations at a longer time lag, as evident from the box and whisker plots for the 1-3 m profile (Figure 13).

In general, a strong linear relationship (R>0.5) is found between the LFMC and $SMC_{0\text{-}350mm}$, except for forested locations (Figure 13, light green boxes). The average lag-correlation observed for grasslands, woodlands, forestlands and croplands between LFMC and $SMC_{0\text{-}350mm}$ are 0.73, 0.69, 0.43 and 0.57, respectively. The corresponding average lag is 14.28, 64.54, 218.91 and 16.85 days. The forested sites generally display a higher correlation to the thicker, 0-3 m soil profile. This is likely a consequence of the deeper roots typical of over-story forest canopies which can draw water from a much thicker soil profile than the 0-350 mm layer. However, the skill lost by using the 0-350 mm profile instead of the 0-3 m is not overly large and the difference in mean correlation is only 0.02.

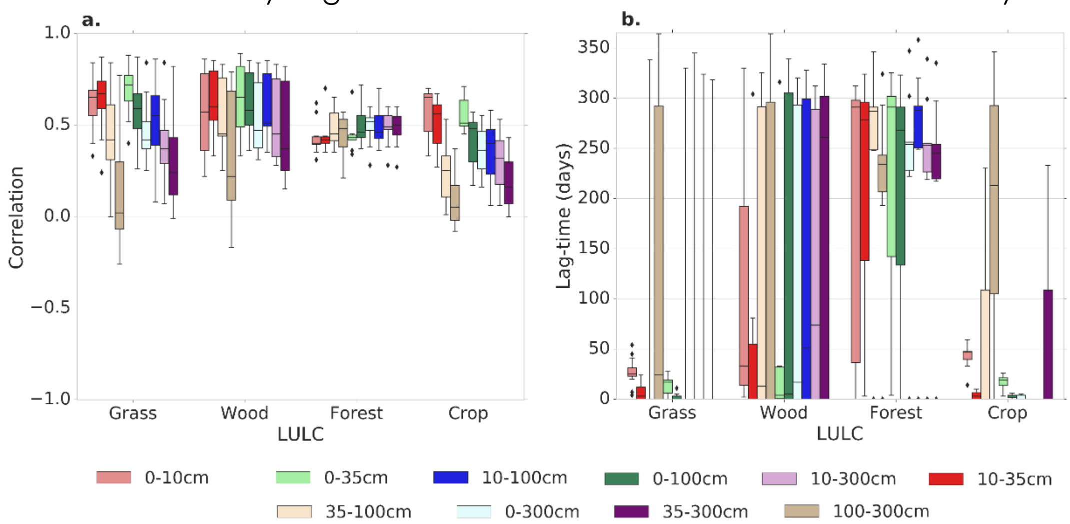

FIGURE 13. BOX AND WHISKER PLOT REPRESETING A) LAG-CORRELATION AND B) LAG IN DAYS BETWEEN LFMC AND SM FROM VARIOUS JASMIN NATIVE AND DERIVED LAYERS. THE GROUPING IS DONE BASED ON THE LAND COVER TYPE OF THE OBSERVING SITE/ THE OUTLIERS ARE MARKED AS DIAMONDS.

LFMC predictive model

The predictive model returned an average R^2 of 0.70 and an RMSD of 14.1% over the 60 sites for the training period. The fit varies with location and the R^2 obtained ranges from 0.21 to 0.89. There are only 11 sites with an $R^2 < 0.5$ out of the total 60. This is quite encouraging given the simplicity of the modelling approach used here. A variety of reasons could cause the lack of fit observed at a specific location including, but not limited to, data representativity, LFMC and SM model parameter uncertainty, driving and ancillary data errors, and LFMC and SM model physics limitations. An example of a site where the model fit is reasonably good is the Cumberland Plain site (33.6152°S, 150.7236°E) in central New South Wales (Figure 14a). The R^2 obtained at this site is 0.62 with an NRMSD of 13%. The mean ± standard deviation obtained from the AFMS time series over Cumberland Plain is 108.26%±25%. The corresponding value for the predictive model is 107.99%±19.87%.

One of the locations where there is a distinct lack of fit between the modelled and AFMS LFMC is over the Warra site (coordinates: 43.0950°S, 146.6545°E) in southern Tasmania (Figure 14b). The Warra site is located in a wet Eucalyptus forest and is situated in a temperate climate zone. The R^2 and NRMSD obtained over Warra are 0.25 and the NRMSD 13.2% respectively. The sample mean ± standard deviation values for AFMS and modelled LFMC obtained are 111.45%±9.71% and 111.5%±4.83% respectively. That is, the variance in the AFMS dataset is about 4 times that in the modelled one. A repercussion of this high noise in the AFMS dataset is that it can influence the quality of the annual cycle estimated by the model. It is observed that the sites where the AFMS LFMC are very noisy have a poor model fit. In the case of Warra, the annual model could only capture 24% variance in the AFMS time series. Compared to this, the annual model over Cumberland Plains captured 36% of the variance in the AFMS LFMC time series. Further, on the wetter side of the distribution (i.e., first quadrant of the residual scatter plot), the AFMS LFMC shows larger variability than the SM (see Supplementary Figure 1). This possibly highlights controls on daily LFMC dynamics other than the SM in the 0-350 mm profile and which is not represented here. Hence, the specified linear relationship may not be adequate to capture these variations seen in residual LFMC. It is also worth noting that Warra is one of the sites where the JASMIN soil moisture has a low skill (Vinodkumar and Dharssi, 2019). Hence, a combination of factors may have contributed to the bad fit over Warra.

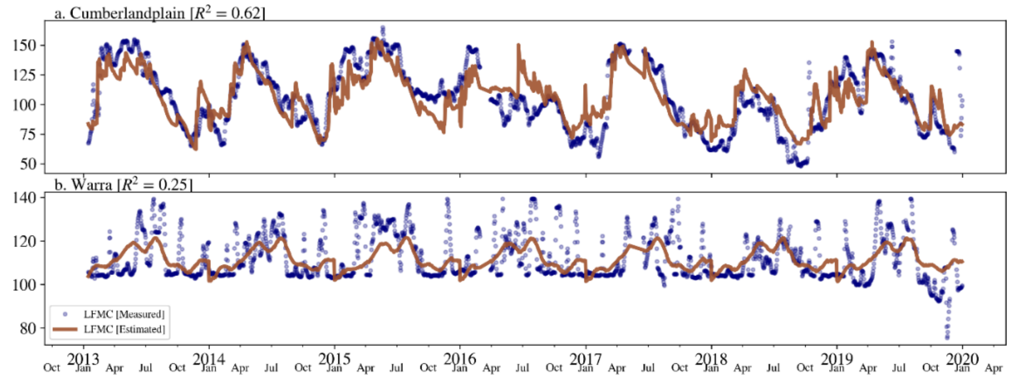

FIGURE 14. TIME SERIES OF MODELLED (LIGHT RED LINE) AND MEASURED (BLACK DOTS) LFMC OVER CUMBERLAND PLAIN AND WARRA SITES. THE CUMBERLAND PLAIN STATION LOCATED IN DRY SCLEROPHYLL FOREST IN THE HAWKESBURY VALLEY IN CENTRAL NEW SOUTH WALES. THE WARRA SITE IS LOCATED IN A WET EUCALYPTUS FOREST AND IS SITUATED IN A TEMPERATE CLIMATE ZONE IN SOUTHERN TASMANIA.

The time function model to estimate the annual cycle and the ordinary least squares regression model to estimate the daily variations are computed separately and then combined to estimate the LFMC value at each 5 km grid point. To check the adequacy of the predictive model, correlation, bias, and normalised root mean squared difference (NRMSD) are computed against the original AFMS dataset for the training period. The NRMSD score is computed by normalising the RMSD using the range of the measured LFMC. The spatial distribution of the resultant correlation and NRMSD scores are presented in Figure 15. A strong correlation is observed over the tropical, northern savannas and southern grasslands and croplands (Figure 15a). The model is found to be generally unbiased (not shown). The random error in the model is usually less than 25% of the dynamic range as indicated by the NRMSD score (Figure 15b).

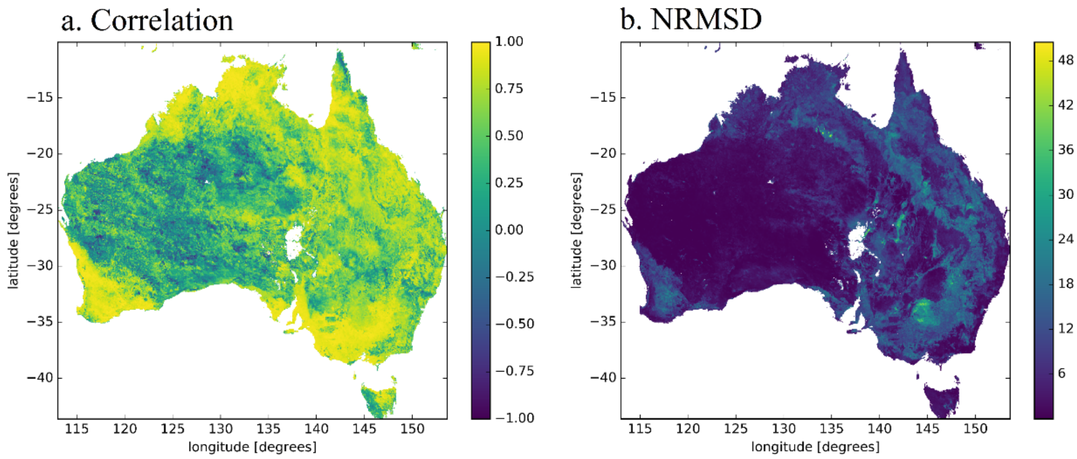

FIGURE 15. VALIDATION OF THE LFMC PREDICTIVE MODEL: A) PEARSON'S PRODUCT-MOMENT CORRELATION, AND B) NORMALISED RMSE

The results indicate that SM is a leading indicator of LFMC. This has significant operational implications as daily variations in LFMC can be predicted using SM information from JASMIN on a national scale. JASMIN is currently run as a prototype, research system with SM analysis done at near-real-time. However, JASMIN can be extended to run both at real-time and in a prognostic mode. The prognostic mode can provide SM forecasts for up to 10 days. The model developed here considers a lag of 14 days between SM and LFMC. This implies a lead time of 14 days for predicting the LFMC estimates and a maximum lead time of 24 days for a 10-day SM forecast product.

This preliminary research was undertaken to understand the relationship that exists between the AFMS LFMC and JASMIN SM products. In that respect, we kept the modelling strategy fairly simple. For example, the model considers only a single soil profile and lag value at all locations across the country. The correlation analysis indicates that the dependence of LFMC to SM can vary with vegetation type. For a plant with complex, deeper root systems, the relationship may exist at multiple soil layers. Also, the lag between the two variables is an attribute of the location determined by a range of factors including soil and vegetation characteristics. Therefore, the future modelling strategy may consider a spatially varying lag as well as a combination of soil layers.

KEY MILESTONES

1. Comparison of KBDI and SDI against NWP soil moisture analysis.
2. Presentation at 2016 AFAC Conference.
3. Published a paper as co-authors in Remote Sensing of the Environment journal.
4. Published a paper in Water Resources Research.
5. Development of the JASMIN system.
6. Bureau of Meteorology seminar on the development and evaluation of the JASMIN system.
7. Bureau of Meteorology research report on the JASMIN system.
8. Presentation at 2018 AFAC conference.
9. Developed JASMIN calibrated products.
10. JASMIN made available through Bureau's THREDDS server and AFMS.
11. Developed a Bureau internal web interface to visualise JASMIN data.
12. Bureau of Meteorology seminar on JASMIN calibration.
13. Developed JASMIN downscaled products.
14. Technical report on validation of the downscaled JASMIN product.
15. Bureau of Meteorology on JASMIN downscaling.
16. Published a paper in Agriculture and Forest Meteorology journal.
17. Presentation at 2019 AFAC conference.
18. Development of a simple model to predict live fuel moisture using JASMIN soil moisture information.
19. Bureau research seminar on the live fuel moisture – soil moisture relationship.
20. Technical report on the live fuel moisture – soil moisture relationship.

UTILISATION AND IMPACT

SUMMARY

In light of the lack of a comprehensive system to analyse soil moisture accurately for fire prediction, a stand-alone high-resolution land surface modelling system has been developed. The new system is called JASMIN and the core focus during its development has been on the utilization pathways. In that respect, the project developed several outputs, a list of which is given below.

a) High-resolution KBDI and SDI datasets – 1970 onwards, updated NRT and available via an internal web server.

b) JASMIN volumetric soil moisture – 2010 onwards, updated NRT, available via BoM THREDDS and AFMS.

c) Calibrated JASMIN soil dryness – total 8 products with varying characteristics, designed to accommodate specific user need and application: 2010 onwards, updated NRT, available via BoM THREDDS server

d) Downscaled JASMIN surface volumetric water content at 1 km spatial resolution.

e) An LFMC product developed using a simple predictive model based on soil moisture.

JASMIN

Description

JASMIN is a national scale, high-resolution soil moisture analysis produced daily at 5 km resolution. JASMIN provides soil moisture information in the form of volumetric soil moisture content ($m^3\ m^{-3}$), which represent the volume of moisture in a unit volume of soil. JASMIN computes volumetric soil moisture at 4 soil layers, with thicknesses of 100 mm, 250 mm, 650 mm and 2 m. Thus, the soil column in JASMIN is 3 m deep.

Extent of use

- JASMIN assessed in WA DBCA study on tall wet forest fuel availability, with initial indications that it will prove useful in that setting.
- Tas Parks and Wildlife using JASMIN as one of the decisions supports tools to restrict the use of open fires in national parks.
- JASMIN data updated specifically to assist with Tasmanian decision-making for 2018-19 seasonal bushfire assessment workshop and preseason consultative committee on fire weather.

Utilisation potential

- There is continuing interest in the application of the JASMIN system to the Australian Fire Danger Rating System ongoing work and approaching operational implementation.
- Currently discussing opportunities to combine best features of AWRA-L hydrological modelling project (and website) and JASMIN to deliver a single, improved and unified Bureau Land Dryness product.

Utilisation impact

- Experience from JASMIN was drawn upon to develop an offline system to initialise Bureau of Meteorology's new seasonal forecasting system, ACCESS-S1.
- A manuscript has been submitted to the Geophysical Research Letters journal titled " Characterising the 2019-2020 Australian bushfires using SMAP vegetation optical depth retrievals". This research is done in collaboration with NASA Goddard's LIS team (who lead the research) and utilises JASMIN (referenced below).

Description

1. Dharssi, I., and Vinodkumar, 2017, JASMIN: A prototype high-resolution soil moisture analysis system for Australia, *Bureau Research Reports*, No. 026.
2. JASMIN daily volumetric soil moisture data available via the Australian Flammability and Monitoring System (AFMS) - (e.g.: http://wenfo.org/afms/#_/sm/gfe_fire_weather/_/_/_/5/6/2019/_)
3. JASMIN volumetric soil moisture content and calibrated SMD data available through the BoM THREDDS server:
4. http://opendap.bom.gov.au:8080/thredds/catalog/c35ee8d2a475e10ea06d0ad53b46ce2a/JASMIN_land_dryness/catalog.html
5. Kumar, S. V., Holmes, T., Dharssi, I., Vinodkumar, Hain, C., Peters-Lidard, C., 2020: Characterising the 2019-2020 Australian bushfires using SMAP vegetation optical depth retrievals, Geophysical Research Letter (Submitted).
6. Vinodkumar, and I. Dharssi, 2019, Evaluation and calibration of a high-resolution soil moisture product for wildfire prediction and management, Agriculture and Forest Meteorology, 264, 27–39, doi: 10.1016/j.agrformet.2018.09.012.
7. Vinodkumar, I. Dharssi, J. Bally, P. Steinle, D. McJannet, and J. Walker, 2017, Comparison of soil wetness from multiple models over Australia with observations, Water Resources Research, 53, 633–646, doi: 10.1002/2015WR017738.

CONCLUSION

The BNHCRC project on land dryness arrives at a successful conclusion having completed all the milestones set out in the project proposal. The project in total developed 15 products, including the high-resolution (5 km) KBDI and SDI datasets derived using AWAP data. The major work completed as part of the project includes:

- Establishing JASMIN and demonstrating superiority over current soil moisture estimates (SDI and KBDI). This includes running the system with approximately weekly updates.
- Developing calibration techniques to allow currently used McArthur fire danger meter to employ JASMIN data as an input (JASMIN provides volumetric soil moisture information in Kg/m^2 or m^3/m^3; SDI and KBDI provide soil moisture as rainfall deficits in mm, so JASMIN cannot natively input to the McArthur fire danger calculations);
- Developing techniques to downscale JASMIN data from 5 km to 1 km horizontal resolution.
- Developing a simple model to predict LFMC using soil moisture as the input.

The new JASMIN system can address gaps in the present operational methods by providing accurate soil moisture information in different layers. This is highlighted by the good skill provided by JASMIN in estimating soil moisture at both surface and root zone layers. The biggest beneficiaries of the new system will be fire agencies. Further, JASMIN can produce an analysis of land surface fluxes and is a cheap source of products for applications like initialization of regional NWP and seasonal forecasting systems.

The calibrated drought index products based on JASMIN can replace the existing methods with minimal effort. This calibration exercise is an important step towards faster adoption of JASMIN product for operational use. Considering the considerable resources required to adopt any new source of information in operations, the calibration provides an opportunity to make a significant improvement to the existing system with the least effort. However, in the longer term, we envisage the adoption of raw JASMIN soil moisture for operational fire prediction, potentially reducing the loss of information arising from any form of calibration. The new Australian national fire danger rating system is expected to explore how to incorporate raw JASMIN soil moisture into its fuel availability estimation once the initial development and release of the system is complete. In that respect, we also developed a simple model to estimate LFMC from JASMIN soil moisture. The model can predict LFMC 14 days in advance.

The BNHCRC end-users of the JASMIN remains engaged with the project. Western Australia has offered to pilot JASMIN implementation, with strong interest as well from ACT. Tasmanian users already consider JASMIN when making operational decisions e.g. for Parks and Wildlife, when to impose campfire restrictions. Also, it is anticipated by fire managers that JASMIN will be available for inclusion in the AFDRS as both systems mature. Discussions are underway on how to operationalise JASMIN, given the current availability of AWRA. The two systems have been designed for differing purposes and have different vertical resolutions. AWRA already has a well-developed mechanism for delivering daily-updated data to users. AWRA management is amenable to the idea of incorporating JASMIN insights/techniques into its framework. It is not currently clear whether the higher vertical resolution of JASMIN affords an advantage for fire users. Some work is underway by Alex Holmes at NSW RFS to examine MODIS Fire Radiative Power in comparison with both AWRA and JASMIN to determine which layers of both systems provide the best guidance for estimating fire intensity.

NEXT STEPS

JASMIN in NASA-LIS framework

Existing satellite systems such as ASCAT, SMOS, SMAP etc. are valuable sources of soil moisture measurements. The above satellite measurements can be assimilated with the JULES land surface model to provide more accurate, detailed, and confident estimates and forecasts of land dryness. NASA's LIS framework provides a great opportunity to effectively assimilate the different remote sensing observations with land surface models for national scale estimation of soil dryness. Improving the spatial resolution of the JASMIN soil moisture analysis from 5 km to 1 km can also be achieved within LIS. Our future work intends to implement JASMIN in LIS framework thereby providing a pathway for the future development of JASMIN.

PUBLICATIONS LIST

PEER-REVIEWED JOURNAL ARTICLES

1 Vinodkumar, Dharssi, I., Yebra, M., Fox-Hughes, P., 2020, Exploring soil moisture – live fuel moisture relationship on a continental scale, Agriculture and Forest Meteorology (in preparation).

2 Kumar, S. V., Holmes, T., Dharssi, I., Vinodkumar, Hain, C., Peters-Lidard, C., 2020, Characterizing the 2019-2020 Australian bushfires using SMAP vegetation optical depth retrievals, Geophysical Research Letter (Submitted).

3 Vinodkumar and Dharssi, I., 2019, Evaluation and calibration of a high-resolution soil moisture product for wildfire prediction and management, *Agriiculture & Forest Met.*, 264, 27–39, doi: 10.1016/j.agrformet.2018.09.012.

4 Vinodkumar, Dharssi, I., Bally, J., Steinle, P., McJannet, D., and Walker, J., 2017, Comparison of soil wetness from multiple models over Australia with observations, *Water Resources Research*, 53, 633–646, doi: 10.1002/2015WR017738.

5 Holgate, C. M., R. A. M De Jeu, A. I. J. M. van Dijk, Y. Y. Liu, L. J. Renzullo, Vinodkumar, I. Dharssi, R. M. Parinussa, R. Van Der Schalie, A. Gevaert, J. Walker, and D. McJannet, 2016, Comparison of remotely sensed and modelled soil moisture data sets across Australia, *Remote Sensing of Environment*, 186, 479–500.

CONFERENCE PAPERS

1 Vinodkumar, I. Dharssi, and P. Fox-Hughes, JASMIN: A high-resolution soil moisture analysis system for fire prediction, The Australasian Fire & Emergency Service Authorities Council (AFAC) Conference, August 2019, Melbourne, Australia.

2 Vinodkumar and I. Dharssi, Evaluation and calibration of a land surface model-based soil moisture product for fire danger ratings, The Australasian Fire & Emergency Service Authorities Council (AFAC) Conference, September 2018, Perth, Australia.

3 Vinodkumar and I. Dharssi, Soil dryness in fire danger rating: Time for a change in approach? The Australasian Fire & Emergency Service Authorities Council (AFAC) Conference, September 2016, Brisbane, Australia.

4 Vinodkumar and I. Dharssi, Verification of soil moisture from land surface models and traditional soil dryness indices, The Australasian Fire & Emergency Service Authorities Council (AFAC) Conference, September 2015, Adelaide, Australia.

TECHNICAL REPORTS

1 Dharssi, I., and Vinodkumar, 2017, JASMIN: A prototype high-resolution soil moisture analysis system for Australia, *Bureau Research Reports*, No. 026.

2 Vinodkumar, and I. Dharssi, 2017, Downscaling of soil dryness estimates: A short review. *BNHCRC Reports*, No. 353.2017.

3 Vinodkumar and I. Dharssi, 2017, Evaluation of daily SMD used in Australian forest fire danger rating system. *Bureau Research Reports*, No. 022.

4 Vinodkumar and I. Dharssi, 2015, Sources of soil dryness measures and forecasts for fire danger rating. *Bureau Research Report*, No. 009.

TEAM MEMBERS

RESEARCH TEAM

1. Paul Fox-Hughes, Project Lead, Bureau of Meteorology, Hobart.
2. Imtiaz Dharssi, Science Lead, R&D Division, Bureau of Meteorology, Melbourne.
3. Vinod Kumar, Scientist, Research Section, Bureau of Meteorology, Melbourne.
4. Jeff Kepert, Senior Scientist, Research Section, Bureau of Meteorology, Melbourne.
5. Peter Steinle, Senior Scientist, Research Section, Bureau of Meteorology, Melbourne.
6. Beth Ebert, Senior Research Scientist, Research Section, Bureau of Meteorology, Melbourne.
7. Chun-Hsu Su, Scientist, Research Section, Bureau of Meteorology, Melbourne.
8. Andrew Frost, Scientist, Water Division, Bureau of Meteorology, Sydney.
9. Evan Morgan, Manager, Severe Weather, Bureau of Meteorology, Melbourne.

END-USERS

End-user organization	End-user representative	Extent of engagement (Describe type of engagement)
Tasmania Fire Service, Hobart	Mark Chladil	Direct
ACT Parks	Adam Leavesley	Direct
Predictive Services Unit, Queensland Fire and Emergency Services	Andrew Sturgess	Direct
Country Fire Service, South Australia	Rob Sandford	Direct
Department of Fire and Emergency Services, Western Australia	Jackson Parker	Direct
Parks and Wildlife Service, Tasmania	David Taylor	Direct
NSW RFS	Stuart Matthews	Direct
Department of Biodiversity, Conservation and Attractions, Western Australia	Lachie McCaw	Direct
AFAC	John Bally	Direct

REFERENCES

1 Albergel, C., de Rosnay, P., Gruhier, C., Munoz-Sabater, J., Hasenauer, S., Isaksen, L., Kerr, Y., and Wagner, W., 2012: Evaluation of remotely sensed and modelled soil moisture products using global ground-based in situ observations, Remote Sensing of Environment, 118, 215–226.
2 Anderson, H.E., 1970: Forest fuel ignitibility, Fire Technology, 6, 312–319.
3 Beringer, J., Hutley, L. B., McHugh, I., Arndt, S. K., Campbell, D., Cleugh, H. A., Cleverly, J., Resco de Dios, V., Eamus, D., Evans, B., and Ewenz, C., 2016: An introduction to the Australian and New Zealand flux tower network–OzFlux, Biogeosciences, 13, 5895–5916.
4 Best, M. J., Pryor, M., Clark, D. B., Rooney, G. G., Essery, R. L. H., Menard, C. B., Edwards, J. M., Hendry, M. A., Porson, A., Gedney, N., Mercado, L. M., Sitch, S., Blyth, E., Boucher, O., Cox, P. M., Grimmond, C. S. B., and Harding, R. J., 2011: The Joint UK Land Environment Simulator (JULES), model description - Part 1: Energy and water fluxes, *Geoscientific Model Development*, **4(3)**, 677–699. doi:10.5194/gmd-4-677-2011.
5 Brocca, L., Hasenauer, S., Lacava, T., Melone, F., Moramarco, T., Wagner, W., Dorigo, W., Matgen, P., Martínez-Fernández, J., Llorens, P. and Latron, J., 2011: Soil moisture estimation through ASCAT and AMSR-E sensors: an inter-comparison and validation study across Europe, Remote Sensing of Environment, 115, 3390–3408.
6 Brocca, L., Zucco, G., Mittelbach, H., Moramarco, T., and Seneviratne, S. I., 2014: Absolute versus temporal anomaly and percent of saturation soil moisture spatial variability for six networks worldwide, Water Resources Research, 50(7), 5560–5576. ISSN 1944-7973. doi: 10.1002/2014WR015684.
7 Brooks, R. H., A. T. Corey, Hydraulic properties of porous media, Hydrology Papers, 3, Colorado State University, Fort Collins, 1964.
8 Busch, F. A., Niemann, J. D., and Coleman, M., 2012: Evaluation of an empirical orthogonal function-based method to downscale soil moisture patterns based on topographical attributes, Hydrological Processes, 26(18), 2696–2709.
9 Corey, D. M., Dunlap, W. P., and Burke, M. J., 1998: Averaging correlations: Expected values and bias in combined Pearson r and Fisher's z transformations, The Journal of General Psychology, 125 (3), 245–261.
10 Cox, P. M., Betts, R. A., Bunton, C. B., Essery, R. L. H., Rowntree, P. R., and Smith, J.: The impact of new land surface physics on the GCM simulation of climate and climate sensitivity, Climate Dynamics, 15(3), 183–203, 1999.
11 Dharssi, I., and Vinodkumar, 2017: A prototype high resolution soil moisture analysis system for Australia, Bureau of Meteorology Research Report, No. 026.
12 Dharssi, I., Steinle, P., and Fernon, J.: Improved numerical weather predictions by using optimised urban model parameter values and satellite derived tree heights, 21st International Congress on Modelling and Simulation, Gold Coast, Australia, 2015.
13 Dorigo, W., Scipal, K., Parinussa, R., Liu, Y., Wagner, W., de Jeu, R., 2010: Error characterisation of global active and passive microwave soil moisture datasets, Hydrology and Earth System Sciences, 14, 2605–2616.
14 Finkele, K., Mills, G. A., Beard, G., and Jones, D. A., 2006: National daily gridded SMDSMD and drought factors for use in prediction of forest fire danger index in Australia, Melbourne, Australian Bureau of Meteorology.
15 Fovell, R. G., Rolinski, T., & Cao, Y., 2015: A simple model for the live fuel moisture of chamise, 5.3, 11th Symposium on Fire and Forest Meteorology, Minneapolis, Minnesota.
16 Frost, A., Ramchurn, A., Hafeez, M., Zhao, F., Haverd, V., Beringer, J., Briggs, P.: Evaluation of AWRA-L: the Australian Water Resource Assessment model, 21st International Congress on Modelling and Simulation, Gold Coast, Australia, 2015.
17 Frost, A. J., Ramchurn, A., and Smith, A. 2016: The Bureau's Operational AWRA Landscape (AWRA-L) Model. Bureau of Meteorology Technical Report.
18 Frost, A. J., Ramchurn, A., and Smith, A. 2018. The Australian Landscape Water Balance model (AWRA-L v6). Technical Description of the Australian Water Resources Assessment Landscape model version 6. Bureau of Meteorology Technical Report.
19 Gellie N. J. H., Gibos K. E., and Johnson K., 2010: Relationship between severe landscape dryness and large destructive fires in Victoria, In X. Viegas (Ed.), VI international conference on forest fire research. Coimbra, Portugal, Associação para o Desenvolvimento da Aerodinamica Industrial.
20 Giglio, L., Descloitres, J., Justice, C. O., and Kaufman, Y., 2003: An enhanced contextual fire detection algorithm for MODIS, Remote Sensing of the Environment, 87, 273–282.
21 Glowacki, T., Xiao, Y., and Steinle, P., 2012: Mesoscale Surface Analysis System for the Australian Domain: Design Issues, Development Status, and System Validation, Weather and Forecasting, 27, 141–157, doi:10.1175/WAF-D-10-05063.1.
22 Haines, D. A., Johnson, V. J., and Main, W. A., 1976: An assessment of three measures of long-term moisture deficiency before critical fire periods, U.S. Department of Agriculture and Forest Services Research Papers, No. NC-131.
23 Hatton, T.J., Viney, N.R., Catchpole, E.A., De Mestre, N.J., 1988: The influence of soil moisture on eucalyptus leaf litter moisture, Forest Science, 34, 292–301.
24 Hawdon, A., McJannet, D., and Wallace, J., 2014: Calibration and correction procedures for cosmic-ray neutron soil moisture probes located across Australia, Water Resources Research, 50, 5029–5043, doi:10.1002/2013WR015138.
25 Holgate, C. M., De Jeu, R. A. M., van Dijk, A. I. J. M., Liu, Y. Y., Renzullo, L. J., Vinodkumar, Dharssi, I., Parinussa, R. M., Van Der Schalie, R., Gevaert, A., Walker, J., and McJannet, D., 2016: Comparison of remotely sensed and modelled soil moisture data sets across Australia, Remote Sensing of Environment, 186, 479–500.
26 Holmes, A., Rüdiger, C., Tapper, N., and Dharssi I., 2016: Improving Fire Risk Estimation through Investigating

Fire Intensity, Moisture and Temperature Anomalies, Abstract GC44B-04, AGU Fall Meeting, San Francisco, California, 12–16 December.
27 Huffman, G. J., Bolvin, D. T., Nelkin, E. J., Wolff, D. B., Adler, R. F., Gu, G., Hong, Y., Bowman, K. P., and Stocker, E. F., 2007: The TRMM Multi-Satellite Precipitation Analysis (TMPA): Quasi-Global, Multiyear, Combined-Sensor Precipitation Estimates at Fine Scales, Journal of Hydrometeorology, 8(1), 38–55. doi:10.1175/JHM560.1.
28 Jones, D. A., Wang, W., and Fawcett, R., 2009: High-quality spatial climate data-sets for Australia, Australian Meteorological and Oceanographic Journal, 58(4), 233.
29 Kaufman, Y. J., Justice, C. O., Flynn, L. P., Kendall, J. D., Prins, E. M., Giglio, L., Ward, D. E., Menzel, W. P., and Setzer, A.W., 1998: Potential global fire monitoring from EOS-MODIS, Journal of Geophysical Research: Atmospheres, 103(D24), 32215–32238.
30 Keetch, J. J., and Byram, G. M., 1968: A drought index for forest fire control, U.S. Department of Agriculture Forest Services Research Papers, No. SE-38.
31 Marsden-Smedley, J. B., 2009: Planned burning in Tasmania: operational guidelines and review of current knowledge. Fire Management Section, Department of Primary Industries, Parks, Water and the Environment, Hobart, Tasmania.
32 McArthur A. G., 1967: Fire Behaviour in Eucalypt Forest, Australian Commonwealth Forestry and Timber Bureau Leaflet, 107, pp. 25.
33 McColl, K. A., Vogelzang, J., Konings, A. G., Entekhabi, D., Piles, M., and Stoffelen, A., 2014: Extended triple collocation: Estimating errors and correlation coefficients with respect to an unknown target, Geophysical Research Letters, 41(17), 6229–6236.
34 Merlin, O., Al Bitar, A., Walker, J. P., Kerr, Y., 2010: An improved algorithm for disaggregating microwave-derived soil moisture based on red, near-infrared and thermal-infrared data, Remote Sensing of the Environment, 114, 2305–2316.
35 Merlin, O., Chehbouni, A. G., Kerr, Y. H., Njoku, E. G., and Entekhabi, D., 2005: A combined modelling and multispectral/multiresolution remote sensing approach for disaggregation of surface soil moisture: Application to SMOS configuration, IEEE Transactions in Geoscience and Remote Sensing, 43(9), 2036–2050.
36 Merlin, O., Escorihuela, M. J., Mayoral, M. A., Hagolle, O., Al Bitar, A., and Kerr, Y., 2013: Self-calibrated evaporation-based disaggregation of SMOS soil moisture: An evaluation study at 3 km and 100 m resolution in Catalunya, Spain, Remote Sensing of the Environment, 130, 25–38.
37 Merlin, O., Rudiger, C., Al Bitar, A., Richaume, P., Walker, J. P., and Kerr, Y. H., 2012: Disaggregation of SMOS Soil Moisture in South-eastern Australia, IEEE Transactions in Geosciences and Remote Sensing, 50(5), 1556–1571.
38 Merlin, O., Walker, J. P., Chehbouni, A., and Kerr, Y., 2008: Towards deterministic downscaling of SMOS soil moisture using MODIS derived soil evaporative efficiency, Remote Sensing of the Environment, 112(10), 3935–3946.
39 Miralles, D., Crow, W., and Cosh, M., 2010: Estimating spatial sampling errors in coarse-scale soil moisture estimates derived from point-scale observations, Journal of Hydrometeorology, 11, 1423–1429.
40 Molero, B., Merlin, O., MALBÉTEAU, Y., Al Bitar, A., Cabot, F., Stefan, V., Kerr, Y., Bacon, S., Cosh, M.H., Bindlish, R., Jackson, T.J., 2016: SMOS disaggregated soil moisture product at 1 km resolution: processor overview and first validation results. Remote Sensing of the Environment, 180, 361–376.
41 Moran, M.S., Clarke, T.R., Inoue, Y., Vidal, A., 1994: Estimating crop water deficit using the relation between surface-air temperature and spectral vegetation index, Remote Sensing of the Environment, 49, 246–263.
42 Mount, A., 1972: The derivation and testing of a soil dryness index using run-off data, Tasmanian Forestry Commission Technical report, Hobart, Tasmania, pp. 31.
43 Nolan, R.H., Boer, M.M., Resco de Dios, V., Caccamo, G., Bradstock, R.A., 2016: Large-scale, dynamic transformations in fuel moisture drive wildfire activity across south-eastern Australia. Geophysical Research Letters, 43, 4229-4238.
44 Peng, J., Loew, A., Merlin, O., Verhoest, N.E.C., 2017: A review of spatial downscaling of satellite remotely sensed soil moisture, Review of Geophysics, 55 (2), 341–366.
45 Piles, M., Camps, A., Vall-Llossera, M., Corbella, I., Panciera, R., Rudiger, C., Kerr, Y.H., Walker, J., 2011: Downscaling SMOS-derived soil moisture using MODIS visible/infrared data, IEEE Transactions on Geoscience and Remote Sensing, 49, 3156–3166.
46 Puri, K., Dietachmayer, G., Steinle, P., Dix, M., Rikus, L., Logan, L., Naughton, M., Tingwell, C., Xiao, Y., Barras, V. and Bermous, I., 2013: Implementation of the initial ACCESS numerical weather prediction system, Australian Meteorological and Oceanographic Journal, 63, 265–284.
47 Qi, Y., Dennison, P. E., Spencer, J., & Riaño, D., 2012: Monitoring live fuel moisture using soil moisture and remote sensing proxies. Fire Ecology, 8(3), 71.
48 Reichle, R. H., and Koster R. D., 2004: Bias reduction in short records of satellite soil moisture. Geophysical Research Letters, 31(19), doi:10.1029/2004GL020938.
49 Sandholt, I., Rasmussen, K., Andersen, J., 2002: A simple interpretation of the surface temperature/vegetation index space for assessment of surface moisture status. Remote Sensing of the Environment, 79 (2-3), 213–224.
50 Simard, M., Pinto, N., Fisher, J. B., and Baccini, A., 2011: Mapping forest canopy height globally with space-borne LIDAR, Journal of Geophysical Research: Biogeosciences, 116, G04021, doi:10.1029/2011JG001708.
51 Smith, A., Walker, J., Western, A., Young, R., Ellett, K., Pipunic, R., Grayson, R., Siriwardena, L., Chiew, F., and Richter, H., 2012: The Murrumbidgee soil moisture monitoring network data set, Water Resources Research, 48, W07701, doi:10.1029/2012WR011976.
52 Stisen, S., Sandholt, I., Norgaard, A., Fensholt, R. and Jensen, K. H., 2008, Combining the triangle method with thermal inertia to estimate regional evapotranspiration – applied to MSG SEVIRI data in the Senegal River basin, Remote Sensing of Environment, 112, 1242–55.

53 Stoffelen, A., 1998: Toward the true near-surface wind speed: Error modelling and calibration using triple collocation, Journal of Geophysical Research, 7755–7766.
54 Tibshirani, R., 1996: Regression shrinkage and selection via the lasso, Journal of Royal Statistical Society. B., 58, 267–288.
55 van Genuchten, M. T., 1980: A closed-form equation for predicting the hydraulic conductivity of unsaturated soils, Soil Science Society of America Journal, 44, 892–898.
56 Vinodkumar and Dharssi, I., 2017: Evaluation of daily SMD used in Australian forest fire danger rating system Bureau of Meteorology Research Reports, No. 022.
57 Vinodkumar and Dharssi, I., 2019: Evaluation and calibration of a high-resolution soil moisture product for wildfire prediction and management. Agricultural and Forest Meteorology, 264, 27-39.
58 Vinodkumar, Dharssi, I., Bally, J., Steinle, P., McJannet, D., and Walker, J., 2017: Comparison of soil wetness from multiple models over Australia with observations. *Water Resources Research*, 53, doi:10.1002/2015WR017738.
59 Werbylo, K. L., and Niemann, J. D., 2014: Evaluation of sampling techniques to characterise topographically-dependent variability for soil moisture downscaling, Journal of Hydrology, 516, 304–316.
60 Wooster, M. J., Zhukov, B., and Oertel D., 2003: Fire radiative energy for quantitative study of biomass burning: Derivation from the BIRD experimental satellite and comparison to MODIS fire products, Remote Sensing of the Environment, 86, 83–107.
61 Yebra, M., Quan, X., Riaño, D., Larraondo, P. R., van Dijk, A. I., & Cary, G. J., 2018: A fuel moisture content and flammability monitoring methodology for continental Australia based on optical remote sensing. Remote Sensing of Environment, 212, 260-272.
62 Yilmaz, M. T., and Crow, W. T., 2014: Evaluation of assumptions in soil moisture triple collocation analysis, Journal of Hydrometeorology, 15(3), 1293–1302.